

1 Widespread functional tradeoffs govern forest response to

2 drought

³ Jacob I. Levine^{*1,2,3} and William R. L. Anderegg^{1,2}

⁴ *Wilkes Center for Climate Science and Policy, University of Utah, Salt Lake City, UT, USA*

²School of Biological Sciences, University of Utah, Salt Lake City UT, USA

³*Department of Biology, Duke University, Durham NC, USA*

Abstract

Widespread drought-driven mortality and productivity loss pose a growing threat to Earth's forests, yet the mechanisms underlying forest vulnerability to drought remain poorly resolved. Theory suggests that competition and coexistence in water-limited systems are mediated by tradeoffs between drought tolerance and resource acquisitiveness, traits that directly influence species' responses to drought. However, the extent to which these tradeoffs structure natural communities is unclear. Using national-scale forest inventory data, we examined the prevalence of drought tolerance–acquisitiveness tradeoffs and their consequences for forest responses to drought. We found these tradeoffs to be widespread and generally stronger than expected from physiological constraints alone, consistent with resource competition theory. Moreover, communities that more closely adhered to these tradeoffs experienced higher growth and lower mortality during drought. Together, these results highlight the importance of functional tradeoffs and community assembly in shaping forest vulnerability to climate change.

Keywords: Functional Traits; Community Assembly; Drought; Mortality; Growth; Climate Change; Competition; Coexistence

Running Title: Functional Tradeoffs and Drought

Abstract Word Count: 142

²⁴ Main Text Word Count: 5,468

Number of References: 66

Number of Figures, Tables, and Text Boxes: 5

Authorship Statement: JIL and WRLA conceived of the study. JIL performed all analyses and wrote the first draft of the paper. WRLA contributed to subsequent revisions.

*jacob.levine@utah.edu; 310.754.6059 (corresponding author)

30 **Introduction**

31 Increases in the magnitude, duration, and frequency of droughts threaten the stability of forests
32 and their role as a net carbon sink (Allen *et al.* 2010; Randerson *et al.* 2025; Reichstein *et al.*
33 2013). Drought impacts on forests are primarily mediated through two related phenomena: (i)
34 mortality induced by hydraulic damage (Williams *et al.* 2013); and (ii) reduced productivity due to
35 stomatal regulation, decreased leaf area, or increased respiration costs (Xu *et al.* 2019). Both these
36 impacts are increasing with climate change, resulting in mass mortality events and reduced biomass
37 production across a wide array of climates and ecosystem types (Allen *et al.* 2010; Anderegg *et al.*
38 2013; Fettig *et al.* 2019; Gazol & Camarero 2022).

39 Both mortality and growth responses to drought are strongly influenced by plant functional traits.
40 Communities that exhibit traits associated with drought tolerance, such as low xylem vulnerability
41 to embolism or deep roots, typically experience less mortality and growth decline during drought
42 (Anderegg *et al.* 2016; Serra-Maluquer *et al.* 2022; Trugman *et al.* 2020). However, drought
43 responses are not only driven by a community's mean traits. Recent research demonstrates that
44 communities with a greater diversity of hydraulic traits are consistently more resilient to drought
45 impacts, exhibiting reduced mortality rates and sustained evapotranspiration during drought, and
46 recovering faster from it (Anderegg *et al.* 2018; Helfenstein *et al.* 2025; Langan *et al.* 2025).

47 Given the central role of functional traits in shaping ecosystem vulnerability to drought, it is
48 essential that we understand the factors that determine trait patterns within a community. One of
49 the predominant forces shaping traits is community assembly, a process of repeated invasions and
50 extinctions through which a large pool of potential species is whittled down to a coexisting subset
51 by both abiotic and biotic pressures (Kraft & Ackerly 2010; Laughlin *et al.* 2012; Lebrija-Trejos *et*
52 *al.* 2010). Understanding community assembly, and its impact on hydraulic traits, may therefore
53 provide important insights into vegetation response to drought, especially as climate change reshapes
54 plant communities over the next century.

55 Recent work suggests that interspecific tradeoffs in plant hydraulic traits mediate community
56 assembly, shaping the functional makeup of plant communities and therefore their vulnerability
57 to drought (Detto *et al.* 2022; Levine *et al.* 2022, 2024, 2025). Specifically, mechanistic models
58 of competition for water and light indicate that biodiversity is maintained by a tradeoff between
59 plants' ability to maintain growth in dry soil conditions and their ability to rapidly accumulate
60 biomass during periods of abundant water (Levine *et al.* 2025). This tradeoff, which is similar to the
61 broader 'conservative–acquisitive' and 'safety–efficiency' tradeoffs (Gleason *et al.* 2016; Manzoni
62 *et al.* 2013; Reich 2014; Wright *et al.* 2004), allows species with divergent water-use strategies
63 to coexist even when competing strongly for shared water and light resources (Levine *et al.* 2022,
64 2025). 'Acquisitive' species perform better when water is plentiful; however, their drought tolerant
65 competitors are able to maintain growth during dry periods when most species are physiologically
66 shut down, ensuring their persistence. While there is reason to believe these tradeoffs would emerge
67 from fundamental allocational constraints, theory suggests that because they are a requirement for

68 coexistence, they will be maintained through community assembly even if there is no underlying
69 physiological basis (Levine *et al.* 2025). Indeed, recent empirical work suggests these tradeoffs
70 are present across species and communities at large scales (Anderegg *et al.* 2024). Yet it remains
71 unclear whether these tradeoffs are widespread within individual plant communities, and if so, what
72 their consequences are for community response to drought.

73 We hypothesize at least two key ways in which a community's adherence to the drought tolerance–
74 acquisitiveness tradeoff might affect mortality and productivity during drought. First, communities
75 with a stronger tradeoff (i.e. steeper tradeoff slope) contain species at both ends of the tolerant-to-
76 acquisitive spectrum, and these differing strategies are likely to succeed under different circum-
77 stances: drought tolerant species may fare better during periods of acute drought stress, whereas
78 acquisitive species may recover faster in the period following drought. As drought incidence and
79 severity increase over long time scales, the presence of both strategies may provide the greatest over-
80 all resilience. This is essentially a two dimensional extension of the classic expectation that diversity
81 provides resilience through 'bet-hedging', much like diversified investments are less sensitive to
82 market fluctuations (Doak *et al.* 1998).

83 The second mechanism through which drought tolerance–acquisitiveness tradeoffs may impact
84 drought response is closely tied to community assembly and resource competition. Communities
85 which more closely adhere to the tradeoff (i.e. exhibit less spread around the tradeoff curve) are likely
86 in an advanced state of assembly. If the tradeoff is a requirement for coexistence, as theory predicts,
87 close adherence to the tradeoff suggests that species lying off it have already been competitively
88 excluded and the existing community should be relatively stable. By contrast, communities that
89 don't closely adhere to the tradeoff may contain species that are in the process of being excluded,
90 for example species which are both less drought tolerant and less acquisitive than their competitors.
91 This could make the community as a whole more vulnerable to competition and environmental stress.
92 Droughts, because they intensify competition for water, can spur a sudden advancement of the
93 community assembly process (White & Jentsch 2004), leading to increased mortality and reduced
94 growth as species lying off the tradeoff are competitively excluded. Indeed, there is substantial
95 evidence that competition plays a key role in community response to drought (Bradford *et al.* 2022;
96 Bradford & Bell 2017; Castagneri *et al.* 2022; Gleason *et al.* 2017). However, prior studies have
97 focused simply on the role of population density in drought response (Bradford *et al.* 2022; Bradford
98 & Bell 2017; Shriver *et al.* 2021), and have not considered how density-dependent drought effects
99 interact with functional composition or tradeoffs.

100 Here we conduct a large-scale analysis of longitudinal forest inventory data to answer the fol-
101 lowing questions: (1) Do communities exhibit a tradeoff between drought tolerance and resource
102 acquisitiveness, and if so, what are the ecological and climatic drivers of this tradeoff? and (2) Are
103 communities that exhibit these tradeoffs more resilient to drought? To answer these questions we
104 take advantage of the U.S. Forest Service's Forest Inventory and Analysis (FIA) Dataset, which
105 tracks the growth and mortality of individual trees through time across forested regions of the U.S.
106 By linking this national-scale inventory data to comprehensive functional trait registries (Choat *et al.*
107 2012; Kattge *et al.* 2011; Knighton *et al.* 2024), we characterize the tradeoffs exhibited by plant

108 communities across a wide array of climates and ecosystem types experiencing elevated drought in
109 the 21st century.

110 **Methods**

111 **Forest inventory and climate data**

112 The United States Forest Service's Forest Inventory and Analysis (FIA) program uses permanent
113 sampling plots to track the size, species, and mortality status of individual trees in forested regions
114 across the United States (Bechtold & Patterson 2005). These plots are remeasured every 5-10 years,
115 depending on region, allowing us to calculate annualized average growth and mortality rates over
116 the interval between samples. FIA plots consist of four subplots with 7.32m (24 ft) radii spaced
117 36.6m apart, and are divided into unique subsections called 'conditions', defined as homogenous
118 areas with similar land use, species composition, stand age, and ownership. All calculations were
119 performed at the condition level to ensure our analysis focused on distinct ecological communities.

120 Prior to processing, all conditions comprising less than 30% of a plot's total area were removed,
121 as smaller areas are unlikely to capture enough individuals to properly characterize a distinct
122 community. In addition, all plots with evidence of fire or harvesting were excluded. We restricted
123 our analysis to the contiguous U.S., excluding data from Alaska, Hawaii, and Puerto Rico. The
124 resulting dataset contained 114,512 unique plots measured across 48 states between 1995 and 2024
125 (Fig. 1). The observations included in the final dataset represent pairs of repeated measurements of
126 these plots at the condition level. For example, if a plot were measured in 2000, 2010, and 2020,
127 two observations were recorded: 2000-2010 and 2010-2020. For each observation, we calculated:
128 1) the annualized average basal area growth rate and 2) the annualized average mortality rate (in
129 units of trees per acre, TPA) during the interval between measurements. Data on total trees per acre,
130 basal area, stand age, species composition, species richness, and relative abundance (TPA) of each
131 species were also recorded for the first measurement in each pair.

132 To characterize long-term average climate, we calculated mean annual temperature (MAT) and
133 mean annual precipitation (MAP) from 1961-2020 using data from TerraClimate (Abatzoglou *et al.*
134 2018). We additionally extracted monthly observations of the Palmer drought severity index (PDSI)
135 to determine the severity of drought for each year in the dataset (1995-2023). After aggregating
136 these monthly observations to an annual scale, two drought metrics were established: (i) average
137 drought strength—defined as the mean PDSI of years with PDSI < -2, a common threshold for
138 drought incidence (Maule *et al.* 2013)—and (ii) drought burden, defined as the proportion of the
139 inter-sample period with PDSI < -2.

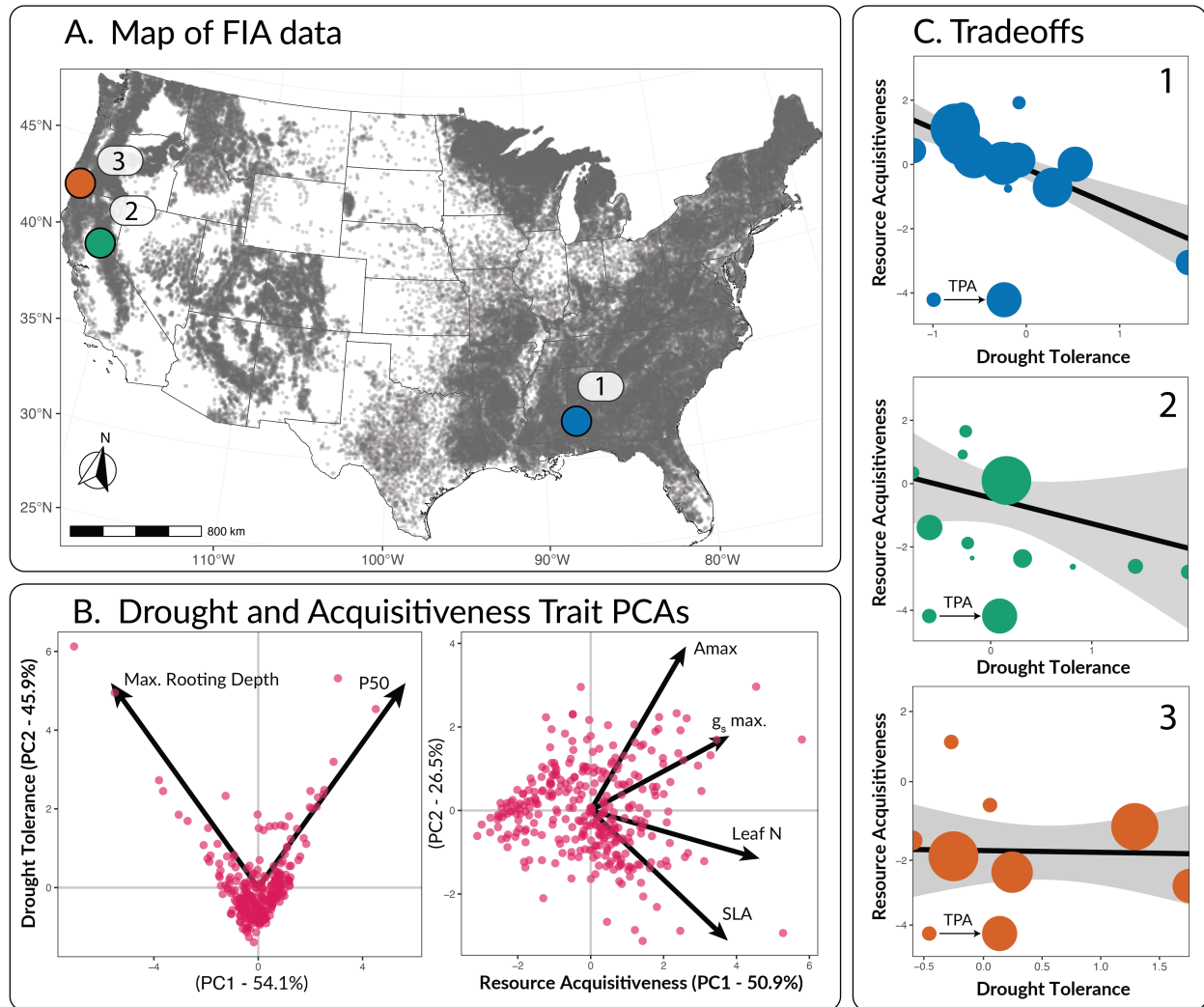


Figure 1: Study overview. (A) Map of FIA plot locations, where each dot represents a single FIA plot. Data from plots labelled 1, 2, and 3, are displayed in panel C. (B) Principle Component Analyses used to characterize species' drought tolerance and resource acquisitiveness. The left panel shows the PCA for drought tolerance traits, where the y axis, PC2, is used as the drought tolerance index in panel C, as increases in PC2 correspond to increased rooting depth and xylem resilience to embolism (P_{50}). The right panel shows the PCA for acquisitiveness traits, where PC1 is used at the resource acquisitiveness index as it corresponds to increases in maximum photosynthetic rate (A_{max}), maximum stomatal conductance ($g_{s,max}$), leaf nitrogen content, and specific leaf area (SLA). (C) Example community-level tradeoffs between drought tolerance and resource acquisitiveness. Each panel corresponds to a single FIA plot (panel A), and are sorted in decreasing order of tradeoff slope. Points represent individual species, and the size of each point corresponds to the trees per acre (TPA) of that species within the plot. Black lines represent TPA-weighted regression slopes, and gray areas represent 95% confidence intervals.

140 Quantifying functional tradeoffs

141 To characterize functional tradeoffs within FIA conditions, we first mapped each species along
142 gradients of drought tolerance and resource acquisitiveness using six commonly available functional
143 traits: xylem vulnerability to embolism (P_{50}) and maximum rooting depth for drought tolerance,
144 and maximum photosynthetic rate (A_{max}), maximum stomatal conductance ($g_{s,max}$), leaf nitrogen
145 content, and specific leaf area (SLA) for resource acquisitiveness. We obtained data on four of these
146 traits ($g_{s,max}$, maximum rooting depth, SLA, and leaf nitrogen content) from a recently published
147 global dataset of hydraulic and functional traits (Knighton *et al.* 2024). To supplement this dataset,
148 we also pulled direct observations of A_{max} and P_{50} from the Xylem Functional Traits (XFT) (Choat
149 *et al.* 2012) and TRY databases (Kattge *et al.* 2011).

150 For species in the FIA dataset without trait observations in either XFT or TRY, we performed
151 phylogenetic imputation using the TrEvol package (Sanchez-Martinez *et al.* 2024) in R version
152 4.4.1 (R Core Team 2013). This method, which is similar to the one used by Knighton et al (2024),
153 employs random forest models to predict missing trait values from observed values of the target trait
154 (i.e. A_{max} or P_{50}), phylogenetic distances (obtained from the Open Tree of Life (Michonneau *et al.*
155 2016)), and values of a third non-target trait used to establish phylogenetic correlations (in this case
156 wood density, also obtained from TRY and XFT; Fig. S2). To test alignment between our imputed
157 dataset and the dataset from (Knighton *et al.* 2024), we compared the values of P_{50} from each,
158 finding relatively close agreement (Fig. S3). We then used principal component analysis (PCA)
159 to reduce the six traits into a single axis each for drought tolerance and resource acquisitiveness,
160 similar to (Langan *et al.* 2025) (Fig. 1). We fit two PCAs, one for the two drought tolerance traits,
161 and one for the four acquisitiveness traits, and then selected the principal component axis that best
162 correlated with the desired combined measure (Fig. 1).

163 Finally, we fit a series of weighted linear regressions to characterize community-level tradeoffs
164 between drought tolerance and resource acquisitiveness. To do so, we iterated through each
165 observation in the dataset, using the PCA mapping to quantify the drought tolerance and resource
166 acquisitiveness of each species present during the first measurement of each observation-pair.
167 Linear regressions were then fit for the relationship between resource acquisitiveness and drought
168 tolerance, weighted by each species' total TPA. The slope and standard error of these fits were
169 recorded to capture the tradeoff strength and uncertainty. To characterize the degree to which each
170 community followed the tradeoff described by this linear fit (hereafter 'tradeoff adherence'), we
171 calculated the average distance of each species from the tradeoff line, again weighted by TPA (SI 1).
172 After extracting data for each observation and quantifying their drought tolerance–acquisitiveness
173 tradeoffs, we aggregated all data to a 0.25° by 0.25° grid, a common approach for mitigating
174 sampling intensity bias and small-scale spatial autocorrelation in FIA data (Anderegg *et al.* 2022b;
175 Stanke *et al.* 2020; Trugman *et al.* 2020) (Fig. S1; SI 2).

176 **Statistical analyses**

177 *Patterns and drivers of functional tradeoffs*

178 To investigate the degree to which forest communities in the contiguous U.S. exhibit tradeoffs
179 between drought tolerance and resource acquisitiveness, we fit a meta-analytic linear regression
180 to estimate the average tradeoff strength within ecoregions, weighted by the inverse variance in
181 tradeoff slope for each grid cell. Ecoregions were defined using publicly available maps from
182 the U.S. Environmental Protection Agency (EPA). For most regions, we used the EPA's level-1
183 ecoregion classifications. However, as over half of the data fell within a single level-1 ecoregion
184 ('Eastern Temperate Forests') we further divided this region using the EPA's level-2 classifications
185 (Fig. S4). To estimate robust standard errors in light of residual spatial autocorrelation, we used
186 spatial block bootstrapping with 200 iterations (Lahiri 2018) (SI 3.1).

187 We then evaluated whether these tradeoffs primarily reflect the outcome of community assembly
188 versus intrinsic species-level constraints. We did so in two ways: (i) by comparing the average
189 tradeoff slope of each ecoregion to the tradeoff observed among all species present in the full dataset,
190 and (ii) by comparing the strength of community-level tradeoffs within regions of varying size, to
191 the strength of the overall tradeoff observed across all species present in that region (see SI 4 for
192 details on characterizing regional tradeoffs). If the tradeoffs observed at the community level are
193 consistently stronger than the overall and regional tradeoffs, it could suggest an important role for
194 community assembly. Alternatively, if the community-level tradeoffs are weaker or indistinguishable
195 from the overall and regional tradeoffs, it would indicate that they arise primarily from intrinsic
196 physiology or broad-scale biogeographic variation rather than interspecific interactions.

197 We next examined how environmental conditions modulate drought tolerance–acquisitiveness
198 tradeoffs by fitting two meta-analytic models, one describing tradeoff strength and one describing
199 tradeoff adherence. Both models assessed relationships with MAP, MAT, and stand age. Tradeoff
200 strength was characterized using a simple Gaussian model, weighted by the inverse variance of
201 the tradeoff slope estimate for each grid cell. Tradeoff adherence, which is strictly positive, was
202 described using a gamma generalized linear model, again weighted by inverse variance (see SI
203 3 for details). All predictors were transformed to standard units before model fitting, and we
204 again used spatial block bootstrapping to estimate robust standard errors in the presence of spatial
205 autocorrelation (SI 3.1; Figure S5)

206 *Impact of functional tradeoffs on forest response to drought*

207 We assessed the consequences of community-level drought tolerance–acquisitiveness tradeoffs for
208 forest mortality during drought by modeling annualized mortality rates as a function of ecological,
209 climatic, and topographic covariates. These included tradeoff strength and adherence, as well as
210 the community weighted mean and range of drought tolerance and resource acquisitiveness, both

211 metrics known to influence drought impacts in prior studies (Anderegg *et al.* 2016; Anderegg *et*
212 *al.* 2018; Langan *et al.* 2025; Serra-Maluquer *et al.* 2022; Skelton *et al.* 2015). To account for
213 systematic differences across the diverse ecoregions, stand histories, and topography covered by
214 FIA, we also modeled the effects of elevation, MAP, MAT, stand age, and initial basal area. Finally,
215 we included both mean drought strength and drought burden in the model to capture the effect of
216 acute drought on mortality.

217 We considered interactions between initial basal area and three covariates — tradeoff strength,
218 tradeoff adherence, and mean drought strength — to investigate how competition might mediate
219 their impacts on drought mortality. We were particularly interested in the interaction between basal
220 area and tradeoff adherence given its correspondence to the second hypothesized mechanism of
221 tradeoff impacts discussed in the introduction, that communities which more closely adhere to
222 the tradeoff are in an advanced state of assembly, and thus more resilient to drought. Assuming
223 a negative main effect of tradeoff adherence, meaning communities that more tightly follow the
224 tradeoff experience less mortality, a negative interaction would indicate that this effect is amplified
225 in more competitive stands. This would be expected if the impact of tradeoffs on drought response
226 were primarily mediated by resource competition.

227 We analyzed these relationships by fitting a zero-inflated beta generalized additive model, which
228 characterizes mortality as a two-part hurdle where the occurrence of non-zero mortality is modeled
229 as a Bernoulli process, and the observed mortality rate given non-zero mortality is modeled using
230 the beta distribution (Ospina & Ferrari 2012). The model was fit using the 'gamlss' package (version
231 5.4-22) in R (Stasinopoulos & Rigby 2007), and all covariates were normalized to standard units
232 before model fitting (SI 5).

233 We employed a similar approach to quantify the impact of functional tradeoffs on growth response
234 to drought, using a Gaussian generalized additive model rather than a zero-inflated beta regression,
235 as negative growth rates were occasionally observed. Growth models were fit using the 'mgcv'
236 package in R (Wood 2001). For more details on modeling approach for both the mortality and
237 growth analyses, including methods for handling residual spatial autocorrelation, and sensitivity
238 analyses, see SI 5 and 6.

239 Results

240 Drought tolerance–acquisitiveness tradeoffs are widespread

241 Community-level tradeoffs between drought tolerance and resource acquisitiveness had clear nega-
242 tive slopes in all but two ecoregions (Fig. 2A). A negative tradeoff slope indicates that species which
243 are drought tolerant tend to be less acquisitive and vice versa. Moreover, of the ten ecoregions with
244 negative tradeoff slopes, nine exhibited tradeoffs that were stronger than the overall tradeoff observed
245 among all species in the dataset (Table S3). Similar patterns were observed when comparing local
246 to regional tradeoffs. When using large radii to define regional species pools, community-level

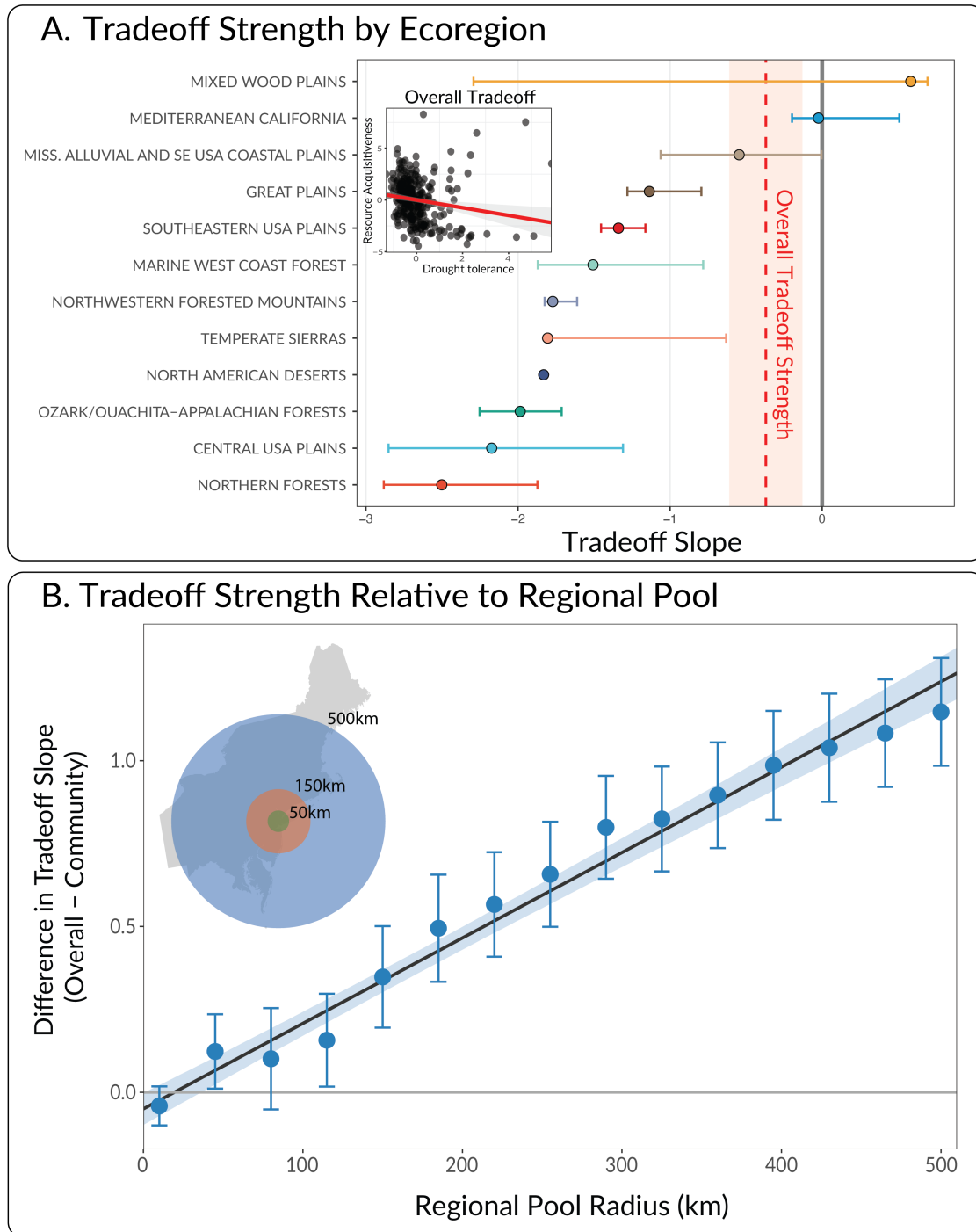


Figure 2: The strength of tolerance–acquisitiveness tradeoffs in U.S. Forests. Panel A shows estimated tradeoff strengths across EPA level 1 and 2 ecoregions in the contiguous United States. Points correspond to the expected mean tradeoff slope, while bars indicate 95% confidence intervals. The dashed red line and shaded area shows the strength of the overall tradeoff and 95% confidence interval calculated for all species in the dataset combined. The inset panel shows the overall tradeoff, where dots correspond to individual species, and the red line indicates the estimated tradeoff. Panel B plots the average strength of local tradeoffs relative to the tradeoff observed among regional species pools. The Y axis is the difference in estimated tradeoff slope between the local community and regional pool, where positive values indicate that the tradeoff was locally stronger (more negative). The X axis is the scale at which the regional species pool is aggregated in kilometers, and the inset contextualizes the size of these pools relative to the northeastern region of the U.S., centered on New York City.

247 tradeoffs were substantially stronger than regional ones (Fig. 2B). As the radius was decreased and
248 the local and regional species pools became more similar, the difference in tradeoff strength between
249 them declined towards zero. However, community-level tradeoffs remained detectably stronger
250 even as they approached parity with regional tradeoffs (Fig. 2B). Together, these results suggest an
251 important role for community assembly in shaping local tolerance–acquisitiveness tradeoffs (Fig.
252 2A,B).

253 Tradeoff strength demonstrated clear associations with MAP, but not temperature or stand age
254 (Fig. 3). Dry grid cells were more likely to exhibit strongly negative tradeoff slopes than wet ones
255 (main effect of MAP: 0.18 [0.04, 0.53]; brackets are 95% Wald confidence intervals). Like tradeoff
256 strength, tradeoff adherence was clearly associated with MAP, with adherence being closer in dry
257 regions than wet ones (0.31 [0.19, 0.41]; Fig. 3). However, MAT also exerted a clear effect on
258 tradeoff adherence, with communities in warm regions more tightly following tradeoffs (-0.29 [-0.38,
259 -0.19]). As with tradeoff strength, the effect of stand age was both small and uncertain (-0.14, [-0.29,
260 0.05]).

261 **Tradeoff adherence, but not strength, is associated with mortality and growth response to**
262 **drought**

263 *Mortality*

264 We observed a clear association between tradeoff adherence and expected annual mortality rate,
265 indicating that communities which more closely adhere to the drought tolerance–resource acquisi-
266 tiveness tradeoff experience less drought mortality (main effect of tradeoff adherence: 0.023 [0.01,
267 0.037]; Fig. 4). However, the effect of tradeoff strength on mortality was both small and uncertain
268 by comparison (0.0055 [-0.007, 0.019]). Neither tradeoff strength nor adherence demonstrated
269 clear interactions with basal area (strength: -0.0026 [-0.014, 0.0087]; adherence: 0.0021 [-0.0095,
270 0.014]).

271 Critically, tradeoff adherence's effect on mortality was similar in magnitude to the effects of
272 both mean drought tolerance and resource acquisitiveness (tolerance: -0.025 [-0.042,-0.0092];
273 acquisitiveness: 0.019 [0.0044, 0.034]), and significantly larger than the effects of trait diversity
274 (range in tolerance: -0.0051 [-0.02, 0.0098]; range in acquisitiveness: 0.0047 [-0.01, 0.02]), each
275 of which are known from past studies to play key roles in plant community response to drought.
276 Intuitively, the estimated effect of mean drought tolerance was negative, indicating that communities
277 with deeper roots and lower xylem vulnerability experienced less drought mortality (Fig. 4).
278 Similarly, communities that exhibited more acquisitive traits experienced elevated drought mortality.
279 Both drought metrics had clear associations with mortality: communities that experienced stronger
280 droughts on average (lower mean PDSI) and higher drought burdens also experienced increased
281 rates of mortality (Fig 4). Finally, we observed a clear, negative interaction between mean drought
282 strength and basal area, suggesting that the effect of drought strength on mortality was magnified in
283 dense stands (Fig. 4). The full model results can be found in Table S6.

Tradeoff Drivers

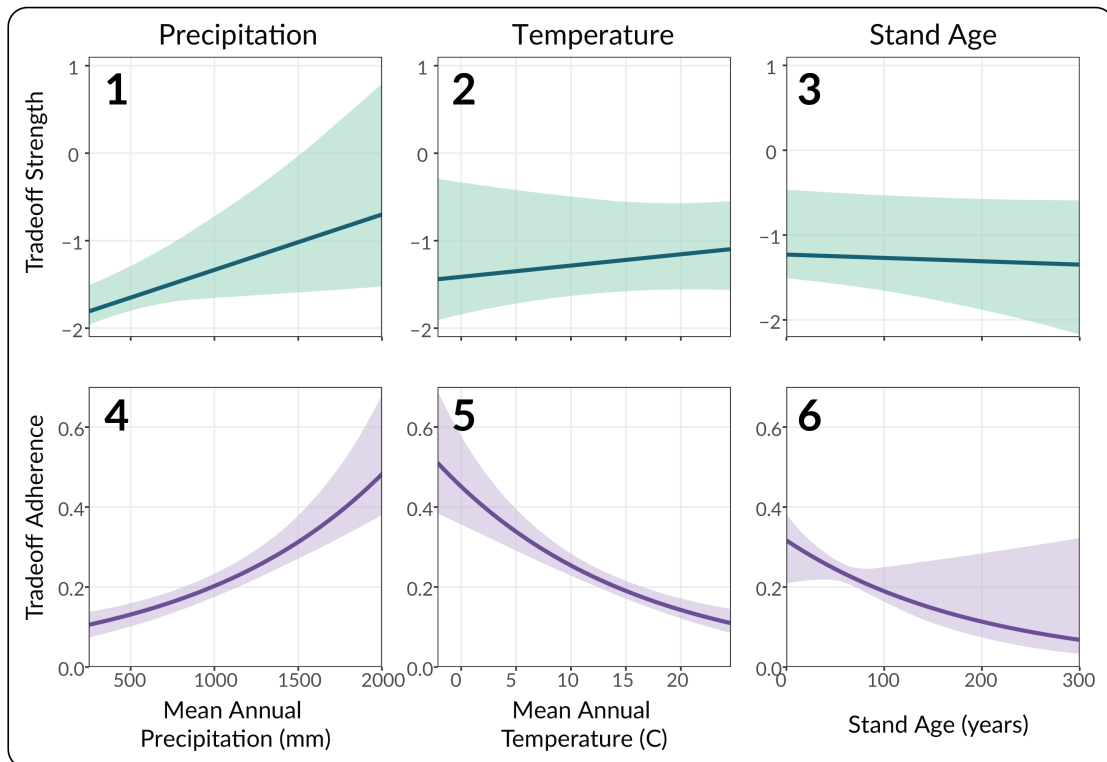


Figure 3: Bioclimatic drivers of tradeoff strength and adherence. Each panel plots the estimated effect of mean annual precipitation (MAP), mean annual temperature (MAT), and stand age on tradeoff strength (1-3) and tradeoff adherence (4-6). Solid lines indicate mean predictions, whereas shaded areas display the 95% confidence intervals for each prediction.

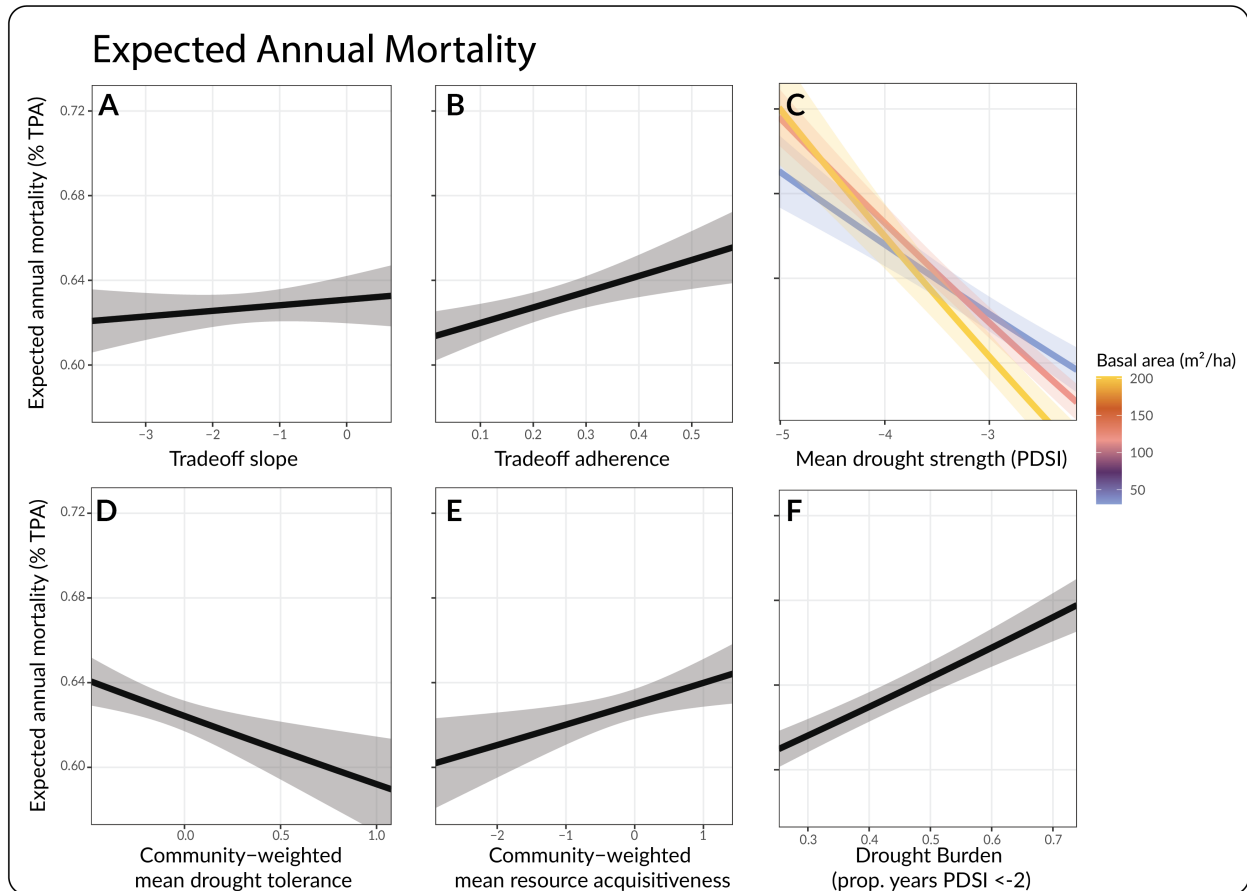


Figure 4: Predicted impacts of tradeoffs, traits, and drought characteristics on mortality. Within each panel, the dark line shows the expected annualized mortality rate (% TPA per year) as a function of six model covariates: tradeoff strength, tradeoff adherence, mean drought strength, community-weighted mean drought tolerance, community-weighted mean resource acquisitiveness, and drought burden (proportion of years experiencing PDSI < -2). Shaded regions indicate 95% confidence intervals, calculated using the delta method. Panel C also shows the interaction between mean drought strength and basal area, where the yellow line indicates prediction under high, red moderate, and blue low basal area.

284 *Growth*

285 Both tradeoff strength and adherence exhibited clear associations with basal area growth rate (Fig. 5).
286 Their effects were negative (strength: -0.018 [-0.03, -0.0058]); adherence:-0.025 [-0.037, -0.013]),
287 indicating that communities with more negative tradeoff slopes, and tighter adherence to those
288 tradeoffs, had higher growth rates during drought than communities with weak tradeoff slopes and
289 adherence. However, the effect of adherence was substantially larger than the effect of strength,
290 especially when accounting for the strong, negative interaction between adherence and basal area
291 (-0.023 [-0.032, -0.014]; Fig. 5). The negative interaction between tradeoff adherence and basal
292 area indicates that the effect of adherence is magnified in dense stands, as would be expected were
293 competitive interactions mediating the impact of tradeoffs on growth response to drought.

294 The effect of mean drought tolerance on growth was both small and uncertain (-0.0067 [-0.02,
295 0.0065]), whereas the effect of mean resource acquisitiveness was clearly negative (-0.026 [-0.043,
296 -0.01]), suggesting that communities with more acquisitive traits were less productive during drought.
297 Similarly, while the effect of range in drought tolerance was small and uncertain (-0.0017 [-0.014,
298 0.01]), communities with a greater diversity of acquisitive traits were less productive (-0.049 [-0.063,
299 -0.036]). Both mean drought strength and drought burden had clear associations with growth rate
300 (strength: 0.035 [0.024, 0.046]; burden: 0.014 [0.0003, 0.027]). Counterintuitively, drought burden
301 had a positive effect, indicating that communities which spent a larger proportion of the time in
302 drought state had higher growth rates (Fig. 5). However, its effect size was small relative to the
303 effect of drought strength (Fig. 5; Table S7).

304 **Discussion**305 *Drought tolerance–resource acquisitiveness tradeoffs*

306 Here we have demonstrated that community-level tradeoffs between drought tolerance and re-
307 source acquisitiveness are both widespread and correlated with mortality and growth response to
308 drought across a wide range of ecosystems and climates, a result with important implications for
309 understanding and predicting forest drought resilience under climate change. A majority of the
310 ecoregions analyzed in this study exhibited tradeoffs that had clear negative slopes, indicating that
311 communities tended to contain species that either had traits associated with drought tolerance (low
312 xylem vulnerability to embolism, deep roots) or traits associated with resource acquisition (high
313 A_{max} , $g_{s,max}$, leaf nitrogen content, SLA; Fig. 2). This finding closely aligns with recent mechanistic
314 community ecology theory that predicts these tradeoffs are a requirement for species coexistence
315 when plants compete for water and light (Levine *et al.* 2024, 2025).

316 The identification of a widespread tradeoff between drought tolerance and resource acquisitiveness
317 echoes prior work on 'conservative–acquisitive' and 'safety–efficiency' tradeoffs in plants (Anderegg
318 *et al.* 2024; Flo *et al.* 2021; Gleason *et al.* 2016; Manzoni *et al.* 2013; Wright *et al.* 2004). The

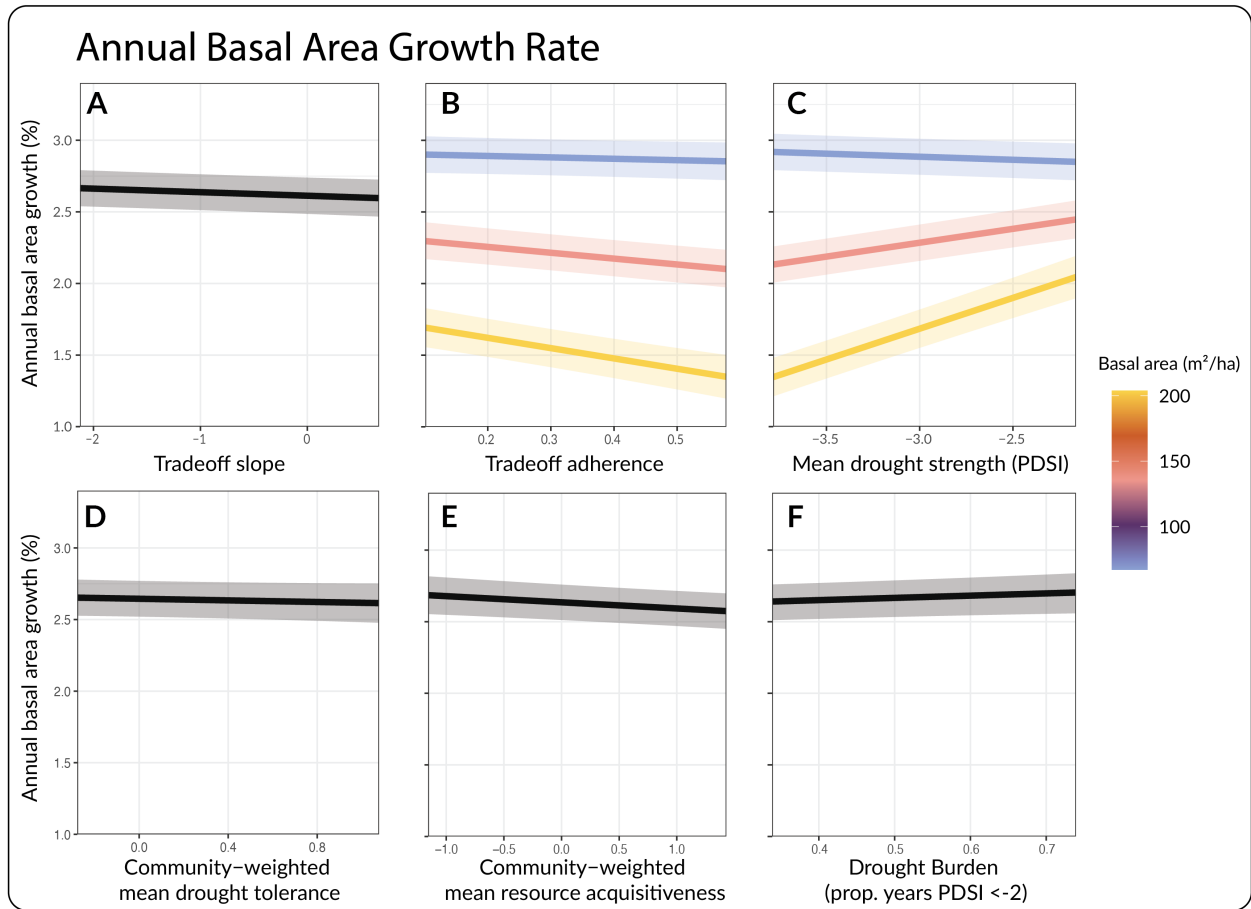


Figure 5: Predicted impacts of tradeoffs, traits, and drought characteristics on growth. Within each panel, the dark line shows the expected annualized basal area growth rate (% basal area per year) as a function of six model covariates: tradeoff strength, tradeoff adherence, mean drought strength, community-weighted mean drought tolerance, community-weighted mean resource acquisitiveness, and drought burden (proportion of years experiencing $PDSI < -2$). Shaded regions indicate 95% confidence intervals. Panels B and C also show interactions with basal area, where the yellow line indicates prediction under high, red moderate, and blue low basal area.

319 conservative–acquisitive tradeoff has been widely observed among plant species globally, and places
320 species along a plant economics spectrum from 'fast' acquisitive species (high SLA, leaf nitrogen
321 content, A_{max}) to 'slow' conservative ones (Wright *et al.* 2004). The safety–efficiency tradeoff is an
322 analogous formulation for hydraulic traits, positing that species trade off investment in xylem safety
323 (reinforced xylem walls, low P_{50}) and efficiency (high maximum stem conductivity)(Flo *et al.* 2021;
324 Gleason *et al.* 2016; Grossiord *et al.* 2020; Tyree *et al.* 1994). The drought tolerance–acquisitiveness
325 tradeoff on which our study is centered is a combination of these two ideas, suggesting that species
326 should specialize either in rapid resource accumulation at the expense of drought tolerance or
327 vis versa. Indeed, the two axes of the tradeoff analyzed here correspond to the safety–efficiency
328 ('drought tolerance' in Fig. 1B,C) and conservative–acquisitive tradeoffs ('acquisitiveness' in Fig.
329 1B,C).

330 *The role of community assembly*

331 As with prior work on safety–efficiency tradeoffs, when all species are considered simultaneously
332 there are very few that are both drought tolerant and acquisitive, reflecting the allocational constraints
333 faced by plants (Fig. 2A, (Gleason *et al.* 2016)). However, there are many species that are neither
334 drought tolerant nor acquisitive, leading to a triangle-shaped distribution of species and relatively
335 weak overall tradeoff (Fig. 2A, (Gleason *et al.* 2016; Grossiord *et al.* 2020)). That tradeoffs
336 appear much stronger at the community level than among all species suggests community assembly
337 may play a key role in selecting species which trade off drought tolerance with acquisitiveness,
338 excluding species which are neither drought tolerant nor acquisitive in relation to the local species
339 pool. This notion is reinforced by the consistency of this finding across spatial scales (Fig. 2B), as
340 local communities exhibit stronger tradeoffs than the regional species pools from which species
341 could plausibly immigrate.

342 The strong positive relationship between MAP and both tradeoff slope and adherence provides
343 additional evidence for the role of community assembly, suggesting that pressures to conform to the
344 tradeoff are stronger in regions where competition for water is more important (Fig. 2). Variation
345 in the regional species pool or environmental pressures could then explain the presence of species
346 which appear to be poor competitors in relation to the global pool of species, particularly if in some
347 systems there is reduced competitive or climatic incentive to invest in the specialized structures
348 and physiology that confer drought tolerance or rapid resource acquisition (Kraft *et al.* 2015; Le
349 Bagousse-Pinguet *et al.* 2017). Indeed, prior work suggests that tradeoffs at the community scale
350 can be obscured at individual, ecosystem, or global scales (Anderegg *et al.* 2024; Lourenço Jr. *et al.*
351 2022; Migliavacca *et al.* 2021).

352 *Tradeoffs and forest response to drought*

353 The strong effect of tradeoff adherence on both mortality and growth response to drought suggests the
354 role of functional tradeoffs in community assembly has downstream effects on ecosystem function
355 and resilience. Communities that exhibited greater spread around the estimated tradeoff curve
356 experienced elevated mortality and reduced growth from drought (Fig. 4, 5). Resource competition
357 theory provides a possible explanation for this pattern: because the tradeoff is a requirement for
358 coexistence, species that lie away from it will eventually be competitively excluded (Levine *et al.*
359 2025). Drought causes heightened competition for water, which might accelerate this competitive
360 exclusion process through mortality or reduced growth in these uncompetitive species. While it is
361 difficult to infer mechanism from noisy observational data, the clear interaction between tradeoff
362 adherence and basal area detected in the model of growth rate supports this explanation. The
363 interaction implies that the effect of tradeoff adherence is stronger in plots experiencing more
364 competition, which would be expected if community assembly were driving the result. However,
365 we did not detect an interaction between tradeoff adherence and basal area in the mortality model.
366 While this finding is consistent with prior studies which indicate that growth is more sensitive to
367 competition than mortality (Shriver *et al.* 2021), a clear link between competition and mortality
368 from drought is still frequently observed in analyses of forest inventory data (Bradford *et al.* 2022;
369 Bradford & Bell 2017; Gleason *et al.* 2017), suggesting that factors other than community assembly
370 may play a role in the relationship between tradeoff adherence and drought mortality.

371 The absence of a relationship between tradeoff strength and drought mortality, and its weak effect
372 on growth, are inconsistent with our hypothesis that communities with stronger tradeoffs would be
373 more resilient to drought (Fig. 4, 5). This hypothesis was based on the notion that communities with
374 stronger tradeoffs would contain both drought intolerant but acquisitive species, and drought tolerant
375 but less acquisitive ones, and that these differing strategies would succeed under different conditions,
376 providing increased community-level resilience. This argument is similar to the explanation for
377 increased drought resilience in communities with greater hydraulic trait diversity, except that it
378 considers two axes of variation in tandem (Anderegg *et al.* 2018; Doak *et al.* 1998; Langan *et*
379 *al.* 2025). Notably, while tradeoff slope is correlated with diversity in both drought tolerance and
380 resource acquisitiveness—the triangle-shaped distribution of species along these two axes means
381 that an increase in the diversity of resource acquisitiveness will typically result in a more negative
382 tradeoff slope—we treat the two as distinct by conditioning mortality and growth on both tradeoff
383 strength and the range in drought tolerance and resource acquisitiveness. Removing these range
384 variables from the models did not result in substantial changes to the estimated effect of tradeoff
385 strength on either growth or mortality (SI 7; Tables S8, S10). Likewise, removing tradeoff strength
386 did not substantially strengthen the weak effects of trait diversity observed in the default models (SI
387 7; Tables S9, S11).

388 The reason for the disagreement between this result and prior studies which demonstrate a clear
389 connection between hydraulic trait diversity and drought resilience is unclear, but may result from
390 the fact that these prior studies were conducted at higher resolutions and with larger plot sizes than

391 the relatively noisy FIA dataset (Anderegg *et al.* 2018; Helfenstein *et al.* 2025; Langan *et al.* 2025;
392 Schnabel *et al.* 2021). If the effect of diversity on drought resilience only emerges at the stand and
393 ecosystem scales, then it is plausible that the small plot-sizes employed by FIA fail to capture these
394 relationships. Regardless, the large discrepancy in effect magnitude between tradeoff strength and
395 tradeoff adherence again suggests that the impact of tradeoffs on drought tolerance is more closely
396 related to community assembly than classic arguments about biodiversity and ecosystem function
397 (Doak *et al.* 1998; Tilman *et al.* 2014).

398 *Limitations*

399 Although we uncover clear and consistent relationships between drought tolerance–acquisitiveness
400 tradeoffs and forest response to drought, several key limitations remain. First, our analysis relies
401 on phylogenetic imputation of functional traits for species without direct measurements in publicly
402 available trait registries (Choat *et al.* 2012; Kattge *et al.* 2011), which introduces uncertainty into
403 downstream estimates of tradeoff strength and adherence, and trait means and ranges. However, the
404 traits we use to quantify functional tradeoffs are highly phylogenetically conserved, especially the
405 hydraulic and leaf morphological traits (Anderegg *et al.* 2022a; Knighton *et al.* 2024; Sanchez-
406 Martinez *et al.* 2020; Ávila-Lovera *et al.* 2023), lending confidence in our ability to impute
407 missing data (Sanchez-Martinez *et al.* 2024). Most of the trait data in our analysis come from
408 a previously published global dataset of imputed functional traits established using models with
409 high out-of-sample predictive ability (Knighton *et al.* 2024). Moreover, the two traits we imputed
410 specifically for this analysis, P_{50} and A_{max} , exhibited strong phylogenetic signal (Pagel's $\lambda = 0.93$
411 [$p < 1e-6$] and 0.47 [$p < 1e-24$], respectively). Second, several of the covariates included in our
412 models of growth and mortality response to drought were collinear, in particular the variables related
413 to functional traits and tradeoffs. However, sensitivity analyses where we permute the models to
414 reduce multicollinearity indicate that these relationships do not qualitatively change the results (SI
415 7). Third, FIA data is inherently noisy owing both to the small plot sizes and location fuzzing.
416 While this is partially offset by spatial upscaling and the large overall sample size, it undoubtedly
417 influences our results, increasing uncertainty and potentially obscuring some relationships which
418 would be detectable in studies with higher fidelity data. Together, these limitations suggest that
419 large-plot investigations, like those used to study the impact of trait diversity on forest response to
420 drought (Anderegg *et al.* 2018; Langan *et al.* 2025; Schnabel *et al.* 2021), should be undertaken to
421 fully understand tradeoffs' role in drought resilience.

422 *Implications for predicting vegetation dynamics under climate change*

423 The magnitude of tradeoff adherence's effect on both growth and mortality was larger than or
424 similar in magnitude to other variables known to play key roles in vegetation response to drought,
425 most notably community weighted mean drought tolerance and resource acquisitiveness, mean

426 annual temperature, and in the case of growth, both mean drought strength and drought burden
427 (Fig. 4, 5; Tables S6, S7). This finding is significant given current predictions for vegetation
428 response to drought and long-term shifts in precipitation and vapor pressure deficit do not account
429 for the ecological dynamics which we suspect underlie this relationship. Dynamic vegetation and
430 earth system models (ESMs) do not accurately capture the functional diversity found in natural
431 communities (Anderegg *et al.* 2022a; Griffith *et al.* 2020; Grossiord 2020; Scheiter *et al.* 2013),
432 in part because they do not incorporate the mechanisms of competition and coexistence which
433 maintain this diversity in nature. Our results suggest that the simplicity of ecological dynamics in
434 these models, which are our best tool for predicting the fate of vegetation over long time scales,
435 may cause them to miss key mechanisms of plant community response to global environmental
436 change. The lack of realistic coexistence dynamics in ESMs has been largely due to the paucity of
437 tractable process-based models of biodiversity maintenance. However, several such models have
438 been developed over the last five years (Dettlo *et al.* 2022; Levine *et al.* 2025), potentially allowing
439 next-generation ESMs to incorporate more detailed treatments of competition that account for the
440 role of tradeoffs in both species coexistence and ecosystem response to drought. Our findings
441 suggest this pursuit could improve forecasting of forest dynamics under climate change.

442 Acknowledgements

443 Funding for this study was provided by the Wilkes Center for Climate Science and Policy's post-
444 doctoral fellowship, as well as the David and Lucille Packard Foundation, the US National Science
445 Foundation grants 2003017, 2044937, and 2330582, and the Alan T. Waterman Award IOS 2325700.
446 We are grateful to members of the Anderegg lab at the University of Utah and Levine lab at Princeton
447 University for helpful feedback and discussions.

448 References

- 449 Abatzoglou, J.T., Dobrowski, S.Z., Parks, S.A. & Hegewisch, K.C. (2018). TerraClimate, a high-
450 resolution global dataset of monthly climate and climatic water balance from 1958–2015.
451 *Scientific data*, 5, 1–12.
- 452 Allen, C.D., Macalady, A.K., Chenchouni, H., Bachelet, D., McDowell, N., Vennetier, M., et al.
453 (2010). A global overview of drought and heat-induced tree mortality reveals emerging climate
454 change risks for forests. *Forest ecology and management*, Adaptation of Forests and Forest
455 Management to Changing Climate, 259, 660–684.
- 456 Anderegg, L.D.L., Griffith, D.M., Cavender-Bares, J., Riley, W.J., Berry, J.A., Dawson, T.E., et
457 al. (2022a). Representing plant diversity in land models: An evolutionary approach to make
458 “Functional Types” more functional. *Global change biology*, 28, 2541–2554.
- 459 Anderegg, W.R., Klein, T., Bartlett, M., Sack, L., Pellegrini, A.F., Choat, B., et al. (2016). Meta-
460 analysis reveals that hydraulic traits explain cross-species patterns of drought-induced tree
461 mortality across the globe. *Proceedings of the national academy of sciences of the united states
462 of america*, 113, 5024–5029.
- 463 Anderegg, W.R.L., Chegwidden, O.S., Badgley, G., Trugman, A.T., Cullenward, D., Abatzoglou,
464 J.T., et al. (2022b). Future climate risks from stress, insects and fire across US forests. *Ecology
465 letters*, 25, 1510–1520.
- 466 Anderegg, W.R.L., Kane, J.M. & Anderegg, L.D.L. (2013). Consequences of widespread tree
467 mortality triggered by drought and temperature stress. *Nature climate change*, 3, 30–36.
- 468 Anderegg, W.R.L., Konings, A.G., Trugman, A.T., Yu, K., Bowling, D.R., Gabbertas, R., et al.
469 (2018). Hydraulic diversity of forests regulates ecosystem resilience during drought. *Nature*,
470 561, 538–541.
- 471 Anderegg, W.R.L., Martínez-Vilalta, J., Mencuccini, M. & Poyatos, R. (2024). Community assembly
472 influences plant trait economic spectra and functional trade-offs at ecosystem scales. *Proceedings
473 of the national academy of sciences*, 121, e2404034121.
- 474 Bechtold, W.A. & Patterson, P.L. (2005). *The enhanced forest inventory and analysis program-national
475 sampling design and estimation procedures*. USDA Forest Service, Southern Research Station.

- 476 Bradford, J.B. & Bell, D.M. (2017). A window of opportunity for climate-change adaptation: Easing
477 tree mortality by reducing forest basal area. *Frontiers in ecology and the environment*, 15, 11–17.
- 478 Bradford, J.B., Shriver, R.K., Robles, M.D., McCauley, L.A., Woolley, T.J., Andrews, C.A., *et al.* (2022). Tree mortality response to drought-density interactions suggests opportunities to
479 enhance drought resistance. *Journal of applied ecology*, 59, 549–559.
- 480 Castagneri, D., Vacchiano, G., Hacket-Pain, A., DeRose, R.J., Klein, T. & Bottero, A. (2022).
481 Meta-analysis Reveals Different Competition Effects on Tree Growth Resistance and Resilience
482 to Drought. *Ecosystems*, 25, 30–43.
- 483 Choat, B., Jansen, S., Brodribb, T.J., Cochard, H., Delzon, S., Bhaskar, R., *et al.* (2012). Global
484 convergence in the vulnerability of forests to drought. *Nature*, 491, 752–755.
- 485 Detto, M., Levine, J.M. & Pacala, S.W. (2022). Maintenance of high diversity in mechanistic forest
486 dynamics models of competition for light. *Ecological monographs*, 92, e1500.
- 487 Doak, D.F., Bigger, D., Harding, E.K., Marvier, M.A., O’Malley, R.E. & Thomson, D. (1998).
488 The Statistical Inevitability of Stability-Diversity Relationships in Community Ecology. *The
489 american naturalist*, 151, 264–276.
- 490 Fettig, C.J., Mortenson, L.A., Bulaon, B.M. & Foulk, P.B. (2019). Tree mortality following drought
491 in the central and southern Sierra Nevada, California, U.S. *Forest ecology and management*, 432,
492 164–178.
- 493 Flo, V., Martínez-Vilalta, J., Mencuccini, M., Granda, V., Anderegg, W.R.L. & Poyatos, R. (2021).
494 Climate and functional traits jointly mediate tree water-use strategies. *New phytologist*, 231,
495 617–630.
- 496 Gazol, A. & Camarero, J.J. (2022). Compound climate events increase tree drought mortality across
497 European forests. *Science of the total environment*, 816, 151604.
- 498 Gleason, K.E., Bradford, J.B., Bottero, A., D’Amato, A.W., Fraver, S., Palik, B.J., *et al.* (2017).
499 Competition amplifies drought stress in forests across broad climatic and compositional gradients.
500 *Ecosphere*, 8, e01849.
- 501 Gleason, S.M., Westoby, M., Jansen, S., Choat, B., Hacke, U.G., Pratt, R.B., *et al.* (2016). Weak
502 tradeoff between xylem safety and xylem-specific hydraulic efficiency across the world’s woody
503 plant species. *New phytologist*, 209, 123–136.
- 504 Griffith, D.M., Osborne, C.P., Edwards, E.J., Bachle, S., Beerling, D.J., Bond, W.J., *et al.* (2020). Lineage-based functional types: Characterising functional diversity to enhance the representation
505 of ecological behaviour in Land Surface Models. *New phytologist*, 228, 15–23.
- 506 Grossiord, C. (2020). Having the right neighbors: How tree species diversity modulates drought
507 impacts on forests. *New phytologist*, 228, 42–49.
- 508 Grossiord, C., Ulrich, D.E.M. & Vilagrosa, A. (2020). Controls of the hydraulic safety–efficiency
509 trade-off. *Tree physiology*, 40, 573–576.

- 512 Helfenstein, I.S., Sturm, J.T., Schmid, B., Damm, A., Schuman, M.C. & Morsdorf, F. (2025).
513 Satellite Observations Reveal a Positive Relationship Between Trait-Based Diversity and Drought
514 Response in Temperate Forests. *Global change biology*, 31, e70059.
- 515 Kattge, J., Díaz, S., Lavorel, S., Prentice, I.C., Leadley, P., Bönisch, G., *et al.* (2011). TRY – a
516 global database of plant traits. *Global change biology*, 17, 2905–2935.
- 517 Knighton, J., Sanchez-Martinez, P. & Anderegg, L. (2024). A global dataset of tree hydraulic and
518 structural traits imputed from phylogenetic relationships. *Scientific data*, 11, 1336.
- 519 Kraft, N.J. & Ackerly, D.D. (2010). Functional trait and phylogenetic tests of community assembly
520 across spatial scales in an Amazonian forest. *Ecological monographs*, 80, 401–422.
- 521 Kraft, N.J.B., Adler, P.B., Godoy, O., James, E.C., Fuller, S. & Levine, J.M. (2015). Community
522 assembly, coexistence and the environmental filtering metaphor. *Functional ecology*, 29,
523 592–599.
- 524 Lahiri, S.N. (2018). Uncertainty Quantification in Robust Inference for Irregularly Spaced Spatial
525 Data Using Block Bootstrap. *Sankhya a*, 80, 173–221.
- 526 Langan, L., Scheiter, S., Hickler, T. & Higgins, S.I. (2025). Amazon forest resistance to drought is
527 increased by diversity in hydraulic traits. *Nature communications*, 16, 8246.
- 528 Laughlin, D.C., Joshi, C., van Bodegom, P.M., Bastow, Z.A. & Fulé, P.Z. (2012). A predictive
529 model of community assembly that incorporates intraspecific trait variation. *Ecology letters*, 15,
530 1291–1299.
- 531 Le Bagousse-Pinguet, Y., Gross, N., Maestre, F.T., Maire, V., de Bello, F., Fonseca, C.R., *et al.*
532 (2017). Testing the environmental filtering concept in global drylands. *Journal of ecology*, 105,
533 1058–1069.
- 534 Lebrija-Trejos, E., Pérez-García, E.A., Meave, J.A., Bongers, F. & Poorter, L. (2010). Functional
535 traits and environmental filtering drive community assembly in a species-rich tropical system.
536 *Ecology*, 91, 386–398.
- 537 Levine, J.I., Levine, J.M. & Pacala, S.W. (2025). Trait diversity in plant communities maintained by
538 competition for water and light. *Ecological monographs*, 95, e70012.
- 539 Levine, J.I., Levine, J.M., Gibbs, T. & Pacala, S.W. (2022). Competition for water and species coex-
540 istence in phenologically structured annual plant communities. *Ecology letters*, 25, 1110–1125.
- 541 Levine, J.I., Pacala, S.W. & Levine, J.M. (2024). Competition for time: Evidence for an overlooked,
542 diversity-maintaining competitive mechanism. *Ecology letters*, 27, e14422.
- 543 Lourenço Jr., J., Enquist, B.J., von Arx, G., Sonsin-Oliveira, J., Morino, K., Thomaz, L.D., *et al.*
544 (2022). Hydraulic tradeoffs underlie local variation in tropical forest functional diversity and
545 sensitivity to drought. *New phytologist*, 234, 50–63.

- 546 Manzoni, S., Vico, G., Katul, G., Palmroth, S., Jackson, R.B. & Porporato, A. (2013). Hydraulic
547 limits on maximum plant transpiration and the emergence of the safety–efficiency trade-off.
548 *New phytologist*, 198, 169–178.
- 549 Maule, C.F., Thejll, P., Christensen, J.H., Svendsen, S.H. & Hannaford, J. (2013). Improved
550 confidence in regional climate model simulations of precipitation evaluated using drought
551 statistics from the ENSEMBLES models. *Climate dynamics*, 40, 155–173.
- 552 Michonneau, F., Brown, J.W. & Winter, D.J. (2016). Rotl: An R package to interact with the Open
553 Tree of Life data. *Methods in ecology and evolution*, 7, 1476–1481.
- 554 Migliavacca, M., Musavi, T., Mahecha, M.D., Nelson, J.A., Knauer, J., Baldocchi, D.D., *et al.*
555 (2021). The three major axes of terrestrial ecosystem function. *Nature*, 598, 468–472.
- 556 Oehlert, G.W. (1992). A Note on the Delta Method. *The american statistician*, 46, 27–29.
- 557 Ospina, R. & Ferrari, S.L.P. (2012). A general class of zero-or-one inflated beta regression models.
558 *Computational statistics & data analysis*, 56, 1609–1623.
- 559 R Core Team, R. (2013). R: A language and environment for statistical computing.
- 560 Randerson, J.T., Li, Y., Fu, W., Primeau, F., Kim, J.E., Mu, M., *et al.* (2025). The weak land carbon
561 sink hypothesis. *Science advances*, 11, eadr5489.
- 562 Reich, P.B. (2014). The world-wide ‘fast–slow’ plant economics spectrum: A traits manifesto.
563 *Journal of ecology*, 102, 275–301.
- 564 Reichstein, M., Bahn, M., Ciais, P., Frank, D., Mahecha, M.D., Seneviratne, S.I., *et al.* (2013).
565 Climate extremes and the carbon cycle. *Nature*, 500, 287–295.
- 566 Sanchez-Martinez, P., Ackerly, D.D., Martínez-Vilalta, J., Mencuccini, M., Dexter, K.G. & Dawson,
567 T.E. (2024). A framework to study and predict functional trait syndromes using phylogenetic
568 and environmental data. *Methods in ecology and evolution*, 15, 666–681.
- 569 Sanchez-Martinez, P., Martínez-Vilalta, J., Dexter, K.G., Segovia, R.A. & Mencuccini, M. (2020).
570 Adaptation and coordinated evolution of plant hydraulic traits. *Ecology letters*, 23, 1599–1610.
- 571 Scheiter, S., Langan, L. & Higgins, S.I. (2013). Next-generation dynamic global vegetation models:
572 Learning from community ecology. *New phytologist*, 198, 957–969.
- 573 Schnabel, F., Liu, X., Kunz, M., Barry, K.E., Bongers, F.J., Bruelheide, H., *et al.* (2021). Species
574 richness stabilizes productivity via asynchrony and drought-tolerance diversity in a large-scale
575 tree biodiversity experiment. *Science advances*, 7, eabk1643.
- 576 Serra-Maluquer, X., Gazol, A., Anderegg, W.R.L., Martínez-Vilalta, J., Mencuccini, M. & Camarero,
577 J.J. (2022). Wood density and hydraulic traits influence species’ growth response to drought
578 across biomes. *Global change biology*, 28, 3871–3882.

- 579 Shriver, R.K., Yackulic, C.B., Bell, D.M. & Bradford, J.B. (2021). Quantifying the demographic
580 vulnerabilities of dry woodlands to climate and competition using rangewide monitoring data.
581 *Ecology*, 102, e03425.
- 582 Skelton, R.P., West, A.G. & Dawson, T.E. (2015). Predicting plant vulnerability to drought in
583 biodiverse regions using functional traits. *Proceedings of the national academy of sciences*, 112,
584 5744–5749.
- 585 Stanke, H., Finley, A.O., Weed, A.S., Walters, B.F. & Domke, G.M. (2020). rFIA: An R package for
586 estimation of forest attributes with the US Forest Inventory and Analysis database. *Environmental
587 modelling & software*, 127, 104664.
- 588 Stasinopoulos, D.M. & Rigby, R.A. (2007). Generalized additive models for location scale and
589 shape (GAMLSS) in R. *Journal of statistical software*, 23, 1–46.
- 590 Tilman, D., Isbell, F. & Cowles, J.M. (2014). Biodiversity and ecosystem functioning. *Annual
591 review of ecology, evolution, and systematics*, 45, 471–493.
- 592 Trugman, A.T., Anderegg, L.D., Shaw, J.D. & Anderegg, W.R. (2020). Trait velocities reveal
593 that mortality has driven widespread coordinated shifts in forest hydraulic trait composition.
594 *Proceedings of the national academy of sciences*, 117, 8532–8538.
- 595 Trugman, A.T., Anderegg, L.D.L., Anderegg, W.R.L., Das, A.J. & Stephenson, N.L. (2021). Why is
596 Tree Drought Mortality so Hard to Predict? *Trends in ecology & evolution*, 36, 520–532.
- 597 Tyree, M.T., Davis, S.D. & Cochard, H. (1994). Biophysical Perspectives of Xylem Evolution: Is
598 there a Tradeoff of Hydraulic Efficiency for Vulnerability to Dysfunction? *Iawa journal*, 15,
599 335–360.
- 600 Venturas, M.D., Todd, H.N., Trugman, A.T. & Anderegg, W.R.L. (2021). Understanding and
601 predicting forest mortality in the western United States using long-term forest inventory data
602 and modeled hydraulic damage. *New phytologist*, 230, 1896–1910.
- 603 White, P.S. & Jentsch, A. (2004). Disturbance, succession, and community assembly in terrestrial
604 plant communities. *Assembly rules and restoration ecology: bridging the gap between theory
605 and practice*, 342–366.
- 606 Williams, A.P., Allen, C.D., Macalady, A.K., Griffin, D., Woodhouse, C.A. & Meko, D.M. (2013).
607 *Temperature as a potent driver of regional forest drought stress and tree mortality*. Nat Clim
608 Chang. Nature Publishing Group.
- 609 Wood, S.N. (2001). Mgcv: GAMs and generalized ridge regression for R. *R news*, 1, 20–25.
- 610 Wright, I.J., Reich, P.B., Westoby, M., Ackerly, D.D., Baruch, Z., Bongers, F., et al. (2004). The
611 worldwide leaf economics spectrum. *Nature*, 428, 821–827.
- 612 Xu, C., McDowell, N.G., Fisher, R.A., Wei, L., Sevanto, S., Christoffersen, B.O., et al. (2019).
613 Increasing impacts of extreme droughts on vegetation productivity under climate change. *Nature
614 climate change*, 9, 948–953.

- 615 Ávila-Lovera, E., Winter, K. & Goldsmith, G.R. (2023). Evidence for phylogenetic signal and
616 correlated evolution in plant–water relation traits. *New phytologist*, 237, 392–407.

617 **1**

618 **Supplementary Information**

619 **1 Calculating Tradeoff Adherence**

620 To quantify the adherence of communities to the linear tradeoff fits, we calculated the bi-directional
 621 average distance of each species in the community from the tradeoff line, weighted by TPA:

$$d_i = \frac{\sum_{j=1}^{N_i} TPA_{i,j} \frac{|\beta_{1,i}x_{i,j} - \beta_{0,i}y_{i,j}|}{\sqrt{\beta_{1,i}^2 + 1}}}{\sum_{j=1}^{N_i} TPA_{i,j}} \quad (1)$$

622 where N_i is the number of species present in observation i , $TPA_{i,j}$ is the total TPA of species j in
 623 observation i , $\beta_{0,i}$ is the intercept of the linear fit for observation i , $\beta_{1,i}$ is the slope of the linear fit,
 624 and $x_{i,j}$ and $y_{i,j}$ are the drought tolerance and resource acquisitiveness of species j in observation i .

625 To quantify uncertainty in tradeoff adherence, we used a Monte Carlo propagation approach based on
 626 the estimated tradeoff intercept and slope and their joint uncertainty for each condition. Specifically,
 627 after fitting a linear model of the drought tolerance–acquisitiveness tradeoff within each condition,
 628 we drew 100 samples of the intercept and slope from a bivariate normal distribution parameterized
 629 by their point estimates and estimated covariance matrix; for each draw, we recalculated tradeoff
 630 adherence and used the standard deviation of these simulated adherence values as the uncertainty
 631 estimate.

632 **2 Spatial aggregation and gridding of data**

633 All data were aggregated to a 0.25° by 0.25° grid before conducting any statistical analyses (Fig. S1).
 634 We did so for three reasons. First, FIA sampling intensity varies widely across the country, with far
 635 more plots per unit forest area in the eastern U.S. than in the west, which could introduce geographic
 636 bias in downstream analyses. Aggregation helps partially correct for this imbalance. Second, to
 637 protect landowner privacy, FIA applies systematic spatial fuzzing to plot coordinates and swaps the
 638 locations of a small fraction of plots (0–10%, depending on the region) with ecologically similar
 639 plots within the same county. Aggregating to a coarser spatial unit reduces the influence of this
 640 location uncertainty. Third, drought mortality and growth are highly spatially autocorrelated. Spatial
 641 aggregation helps diminish the effects of fine-scale spatial autocorrelation. Below, we describe
 642 additional steps taken to address spatial and temporal autocorrelation at broader scales. Aggregation
 643 of FIA data is commonly done in large-scale analyses of demographic rates (e.g. (Anderegg *et al.*
 644 2022b; Stanke *et al.* 2020; Trugman *et al.* 2020)), and is a primary recommendation from the rFIA
 645 package (Stanke *et al.* 2020).

646 To aggregate condition-level data, we first established a 0.25° by 0.25° grid covering the full spatial
 647 extent of the FIA dataset in the contiguous U.S. For each condition measured within a grid cell in a

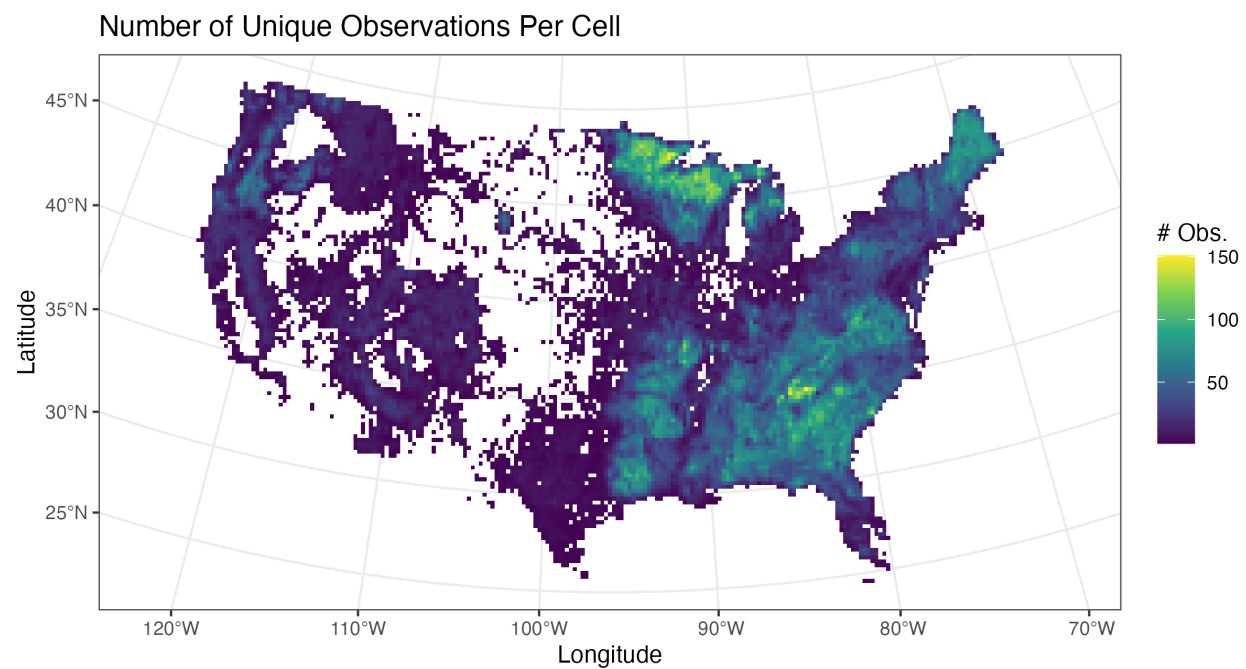


Figure S1: Map of spatially aggregated FIA data, on 0.25° by 0.25° grid. Gridcells are colored by the number of unique observations (condition-years) present in each grid cell.

given year, we computed basal-area-weighted averages of the condition-level variables. For tradeoff slopes we combined plot-level slope estimates within a cell using a two-step precision-weighting procedure that accounts for between-plot heterogeneity (as is done in meta-analysis). For a given cell let β_i and σ_i^2 denote the plot-level slope estimate and its variance, and let BA_i be plot i 's live tree basal area. We first compute the inverse-variance weighted mean:

$$\bar{\beta}_{IV} = \frac{\sum_{i=1}^n w_i \beta_i}{\sum_{i=1}^n w_i}, \quad w_i = \frac{1}{\sigma_i^2},$$

and Cochran's Q :

$$Q = \sum_{i=1}^n w_i (\beta_i - \bar{\beta}_{IV})^2.$$

The between-plot variance is estimated using the DerSimonian–Laird method,

$$c = \sum_{i=1}^n w_i - \frac{\sum_{i=1}^n w_i^2}{\sum_{i=1}^n w_i},$$

$$\tau^2 = \max \left(0, \frac{Q - (n - 1)}{c} \right),$$

where n is the number of valid plot-level estimates within the grid cell. The grid-cell tradeoff slope is then computed as a basal-area-and-inverse-variance–weighted mean,

$$\hat{\beta}_{cell} = \frac{\sum_{i=1}^n \frac{BA_i}{\sigma_i^2} \beta_i}{\sum_{i=1}^n \frac{BA_i}{\sigma_i^2}},$$

while the associated standard error incorporates between-plot heterogeneity by inflating the sampling variances with τ^2 ,

$$SE(\hat{\beta}_{cell}) = \sqrt{\frac{1}{\sum_{i=1}^n \frac{BA_i}{\sigma_i^2 + \tau^2}}}.$$

When a plot contains a single valid plot we report that plot's estimate and its original standard error. Incorporating τ^2 yields a more conservative uncertainty estimate while still using basal-area and inverse variance weighting to quantify the point estimate. Our final dataset therefore contains one

observation for each grid cell in each year with at least one measured plot; e.g. the mortality value for a grid-year is the basal-area-weighted mean mortality experienced by plots in that cell during the preceding sampling interval. MAP, MAT, and drought metrics for each grid cell were computed as the average of all 4km x 4km TerraClimate pixels whose centerpoints fall within the corresponding quarter-degree cell.

3 Quantifying patterns and drivers of drought tolerance – acquisitiveness tradeoffs

Before modeling the variation in tradeoff strength across ecoregions, we first aggregated our data temporally to account for systematic geographic differences in the number of observations per grid cell (Fig. S1). Generally, grid cells in the eastern U.S. contain more measurements, over longer periods of time, than plots in the western U.S. Failing to account for this difference would lead to reduced uncertainty in eastern states, and therefore bias the analysis of geographic patterns and their biophysical drivers. To pool multiple condition-level estimates of tradeoff slope and adherence, we calculated the inverse-variance weighted mean of each, and their uncertainties as $\sqrt{\frac{1}{\sum_i^n \frac{1}{\sigma_i^2}}}$. To assess variation in tradeoff strength across ecoregions, as well as the relationships between tradeoff strength/adherence and MAP, MAT, and stand age, we fit inverse-variance-weighted linear models.

3.1 Accounting for spatial autocorrelation

We detected evidence of significant residual spatial autocorrelation in all three models of tradeoff strength and adherence described above (Fig. S5). To account for this autocorrelation, which can artificially deflate estimates of parameter uncertainty, we implemented a spatial block bootstrap that resamples contiguous spatial units rather than individual observations (Lahiri 2018). For each fitted model, we first estimated the characteristic scale of spatial dependence by computing an empirical variogram of model residuals and fitting a spherical variogram model. The fitted range was used to define the spatial block size. Bootstrap samples were generated by randomly selecting blocks with replacement and including all observations falling within each selected block. Blocks were located by randomly placing centerpoints within the bounding box of the full dataset. Blocks were accumulated until the bootstrap sample contained at least 95% of the original sample size, and samples exceeding 105% of the original size were randomly downsampled to maintain a consistent sample size. For models including categorical predictors, bootstrap samples were required to retain all factor levels present in the original data. Each bootstrap sample was refit using the same weighted regression specification as the original model. Uncertainty in model coefficients was quantified using the bootstrap distributions, with point estimates taken as the predictions of the original model and 95% confidence intervals defined by the 2.5th and 97.5th percentiles in bootstrap samples.

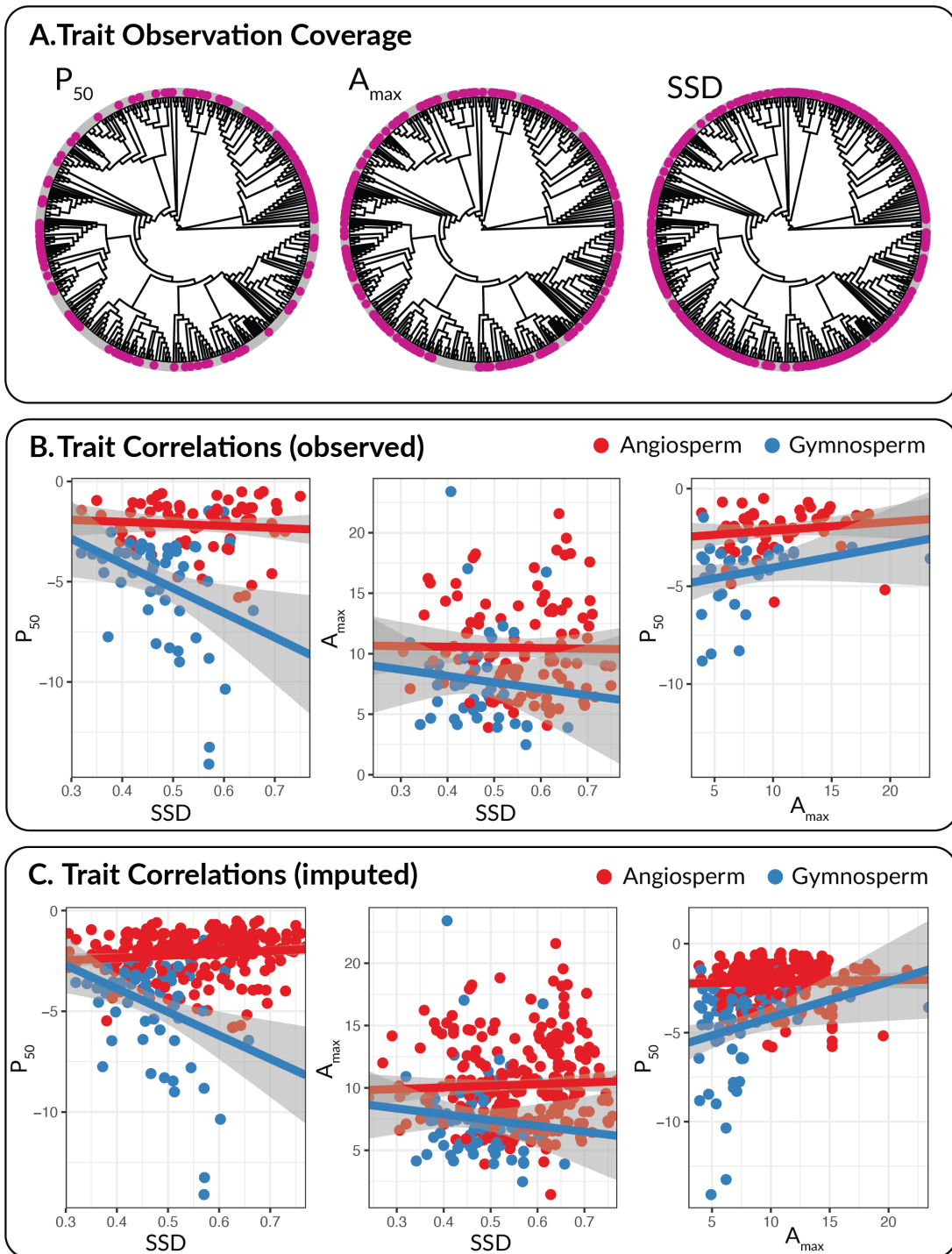


Figure S2: Functional trait coverage and correlations. Panel A shows the phylogenetic coverage of P_{50} , A_{\max} , and specific stem density (SSD). Missing values of both P_{50} and A_{\max} were imputed using phylogenetic relationships and association with SSD. Panel B shows the correlations between these three traits among all observed data, whereas panel C shows the correlations between these three traits using both observed and imputed data. Red points denote angiosperms, while blue points denote gymnosperms.

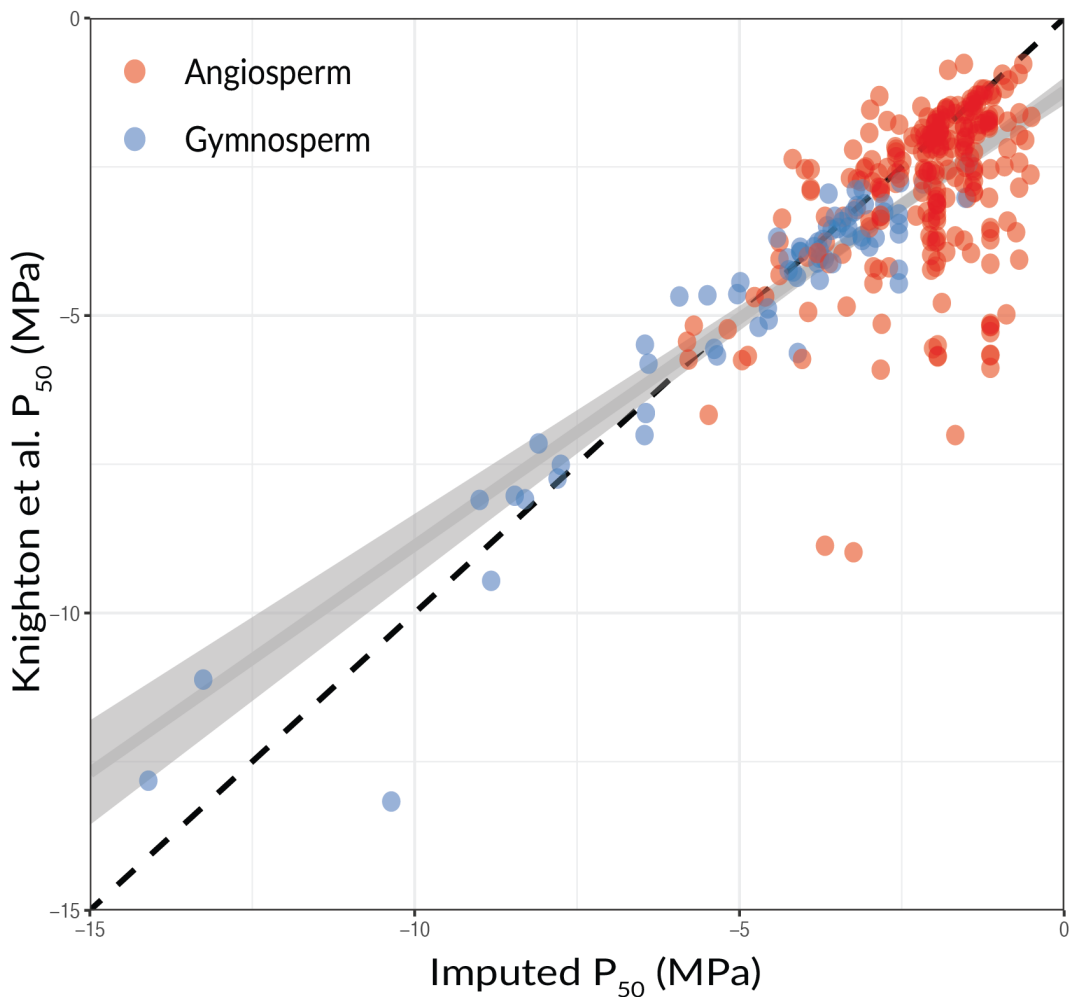


Figure S3: Correlation between values of P_{50} imputed from phylogenetic relationships in our dataset and those imputed by Knighton et al. Dashed line denotes perfect correlation between the two values, while the gray line is a simple linear fit through the points. Species are colored according to whether they are an angiosperm or gymnosperm.

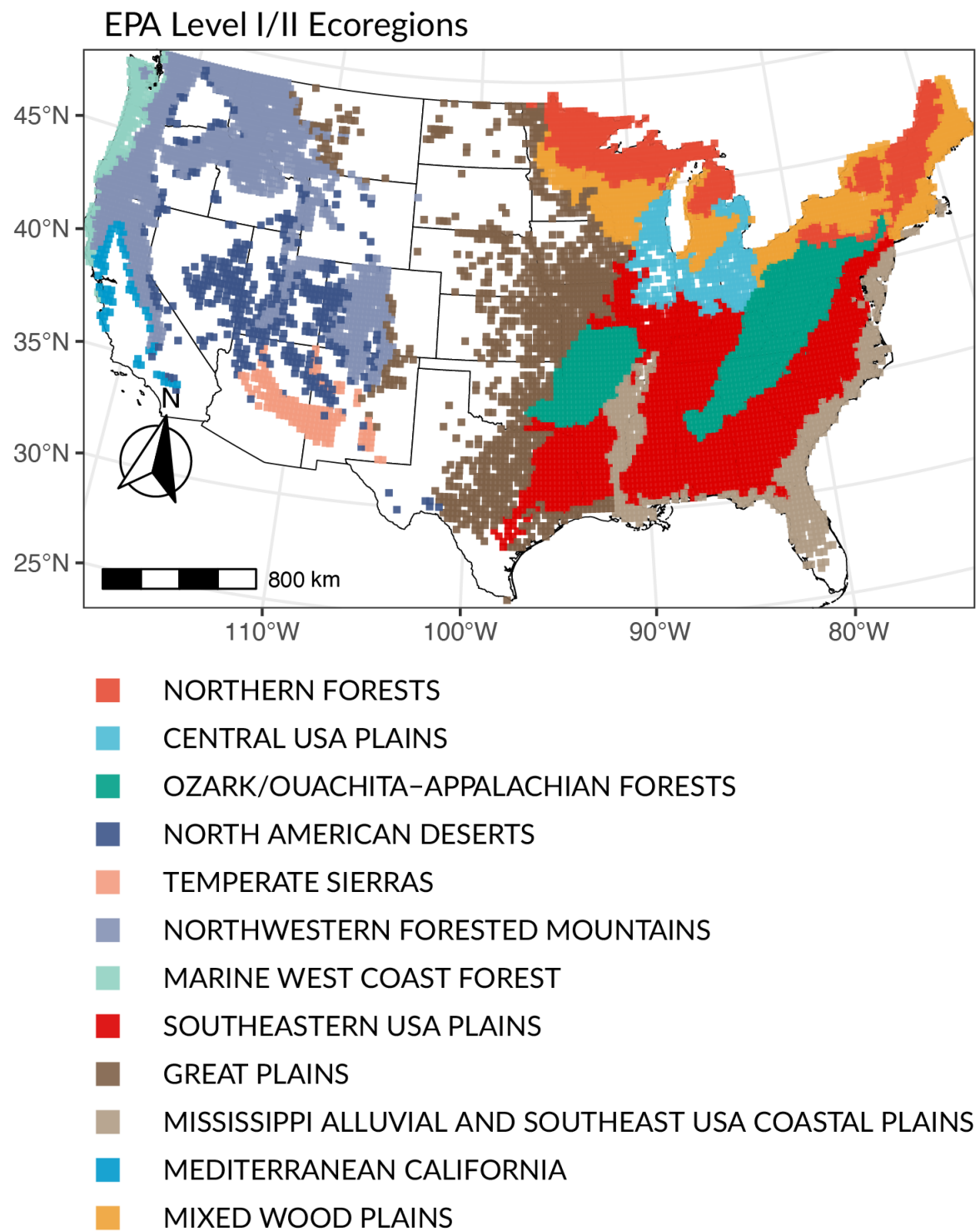


Figure S4: Location of study grid cells within EPA level I/II ecoregions in the contiguous United States.

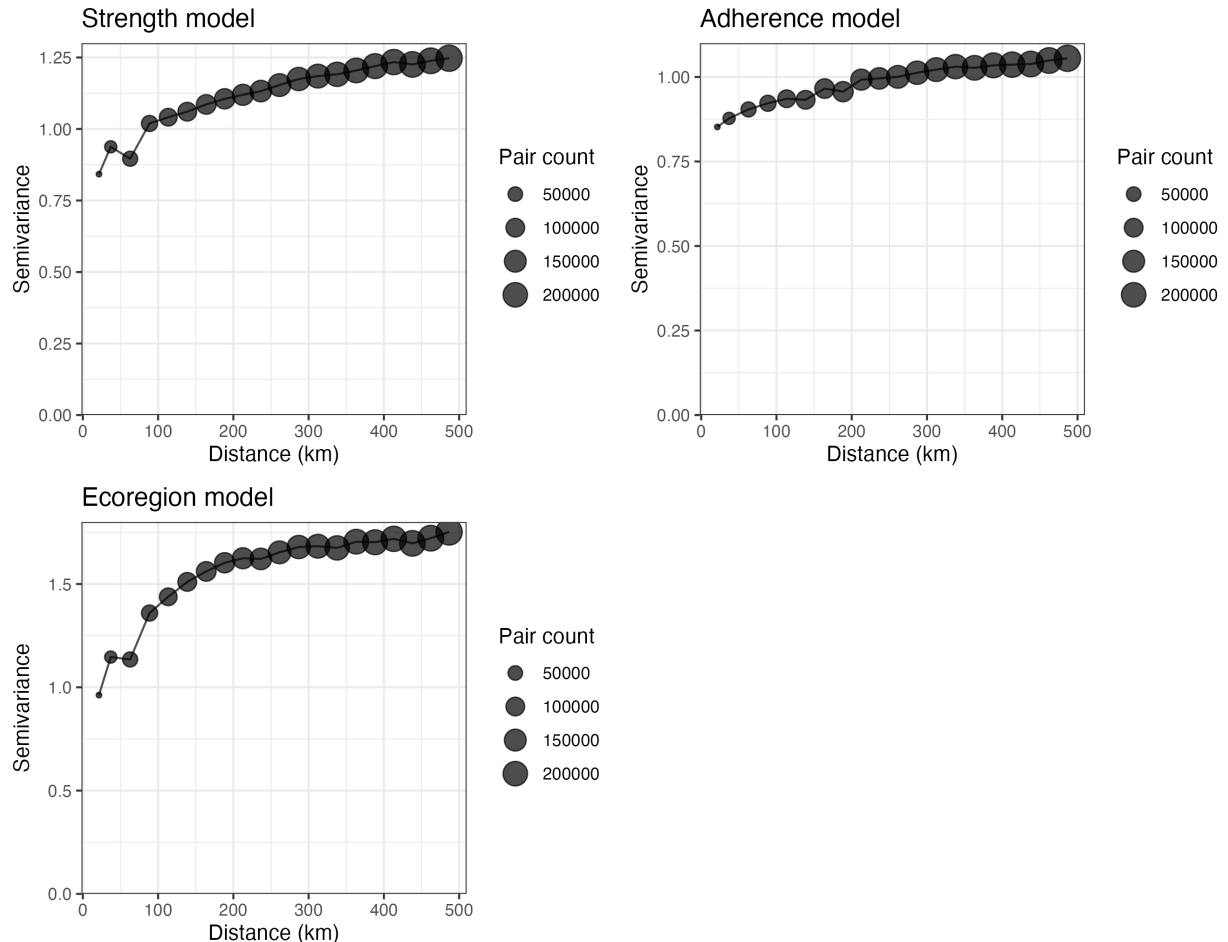


Figure S5: Semivariograms depicting spatial autocorrelation in the residuals of the three meta-analytic models of tradeoff strength and adherence. Increasing trends in semivariance with distance indicate the presence of residual spatial autocorrelation. The size of points refers to the 'pair count' or numbers of unique pairs of observations used in the calculation of semivariance at that distance.

694 **4 Estimating tradeoff strength relative to the regional species pool**

695 In addition to evaluating how average tradeoff strength varies among ecoregions relative to the
 696 overall tradeoff across all species, we examined differences between community-level tradeoffs
 697 and those observed within regional species pools. This comparison provides a more direct test of
 698 community assembly, as broad geographic variation in tradeoff strength among large ecoregions
 699 may reflect processes unrelated to local competition, such as evolutionary history or environmental
 700 filtering. By contrast, comparing community-level tradeoffs to those within the regional species
 701 pool allows us to assess whether tradeoffs at the community scale are stronger than among the set of
 702 species that could realistically disperse into that community. Stronger community-level tradeoffs
 703 would therefore suggest that local competitive interactions exclude geographically proximate species
 704 that might otherwise establish.

705 We further evaluated how the difference between community and regional tradeoff strength varies
 706 with the spatial scale of the regional pool. This difference is expected to be small at local scales,
 707 where community and regional species pools largely overlap, and to increase as the regional pool
 708 expands. A monotonic increase in this difference—particularly if community-level tradeoffs exceed
 709 regional tradeoffs even at modest spatial scales—would provide additional evidence for the role of
 710 community assembly in shaping drought tolerance–resource acquisitiveness tradeoffs.

711 To generate comparisons between community- and regional-scale tradeoffs, we randomly sampled
 712 circular regions with radii ranging from 10 to 500 km. For each radius, we selected 1,000 circular
 713 regions; however, due to the irregular spatial distribution of FIA plots across the contiguous United
 714 States, some regions contained no plots, such that the number of non-empty regions considered at
 715 each radius ranged from approximately 900 to 1,000. Within each circle, tree-level data from all
 716 FIA conditions were pooled, and species abundances were aggregated by summing trees per acre
 717 (TPA) across conditions. We then estimated the slope of the tradeoff between drought tolerance and
 718 resource acquisitiveness at this regional scale using the same methodology described in the main
 719 text.

720 We next estimated the average community-level tradeoff slope within each region while accounting
 721 for both sampling uncertainty and between-plot heterogeneity. Let β_i denote the tradeoff slope
 722 estimated for plot i , with variance σ_i^2 , and let BA_i be the basal area of plot i . We first estimated the
 723 community-level mean tradeoff slope using inverse-variance weighting,

$$\hat{\beta}_{\text{comm}} = \frac{\sum_i w_i \beta_i}{\sum_i w_i}, \quad w_i = \frac{1}{\sigma_i^2}.$$

724 To quantify heterogeneity among plot-level slopes, we computed the Cochran Q statistic and
 725 estimated the between-plot variance τ^2 , again using the DerSimonian–Laird method. The total
 726 variance for each plot-level estimate was then inflated as $\sigma_i^2 + \tau^2$, yielding heterogeneity-adjusted
 727 inverse-variance weights.

We defined two normalized weight vectors over the same set of plots: (i) basal-area weights $a_i = BA_i / \sum_j BA_j$, representing the approximate contribution of each plot to the regional estimate, and (ii) heterogeneity-adjusted inverse-variance weights $b_i = (\sigma_i^2 + \tau^2)^{-1} / \sum_j (\sigma_j^2 + \tau^2)^{-1}$, representing the contribution of each plot to the average community-level estimator. Using these weights, we computed the variances of the regional (r) and community (c) estimators as

$$\text{Var}_r = \sum_i a_i^2 (\sigma_i^2 + \tau^2), \quad \text{Var}_c = \sum_i b_i^2 (\sigma_i^2 + \tau^2),$$

and their covariance,

$$\text{Cov}_{r,c} = \sum_i a_i b_i (\sigma_i^2 + \tau^2),$$

which arises because both estimators are constructed from the same underlying plot-level data. The difference between the regional and community tradeoff slopes for a given circular region was computed as $\hat{d} = \hat{\beta}_r - \hat{\beta}_c$, and its uncertainty was obtained by propagating variance and covariance,

$$\text{SE}(\hat{d}) = \sqrt{\text{Var}_r + \text{Var}_c - 2\text{Cov}_{r,c}}$$

After quantifying \hat{d} and $\text{SE}(\hat{d})$ for each circle of a given radius, we fit a meta-analytic model to estimate the typical difference between community-level and regional tradeoffs for that spatial scale. Finally, to evaluate how the difference in tradeoff slope between community and region varies by region size, we fit a meta-regression for the relationship between \hat{d} and the radius of the regions. All meta-analytic models were fit using the `rma` function in the `metafor` package (version 4.8-0).

5 Modeling mortality response to drought

To assess the relationship between functional tradeoffs and mortality response to drought, we fit a zero-inflated generalized additive model of the following form:

$$\begin{aligned} \text{logit}(v_i) &= \alpha_0 + \sum_k \alpha_k x_{ik}^a + \sum_k f_k^\nu(x_{ik}^b) \\ \text{logit}(\mu_i) &= \beta_0 + \sum_k \beta_k z_{ik}^a \sum_k f_k^\mu(z_{ik}^b) \end{aligned}$$

where v_i is the probability that the observation, y_i , is zero; $\mu_i \in (0,1)$ is the expected mortality rate given $y_i > 0$; α and β are linear coefficients; x_{ik}^a and z_{ik}^a are the values of linear predictor k for the Bernoulli and beta components, respectively; x_{ik}^b and z_{ik}^b are smooth predictors; and $f_k^\pi(\cdot)$ are smooth functions of predictors x_{ik}^b and z_{ik}^b .

Table S1: Mortality Model Specification

Sub-Model	Linear vs. Smooth	Variable
Beta (μ)	Linear	Tradeoff Strength Tradeoff Adherence CWM Drought Tol. CWM Resource Acq. Range Drought Tol. Range Resource Acq. Drought Strength Drought Burden Elevation MAP MAT Stand Age Basal Area Drought Strength x Basal Area Tradeoff Strength x Basal Area Tradeoff Adherence x Basal Area
	Smooth	Latitude Longitude Year
Bernoulli (v)	Linear	Drought Strength Drought Burden Elevation MAP MAT Stand Age Basal Area Drought Strength x Basal Area
	Smooth	Latitude Longitude Year

Because the Bernoulli and beta components of the model are specified separately, the identify of the predictors are allowed to vary. The full specification of the model can be found in Table S1. Our rationale for not including tradeoff and trait metrics in the Bernoulli component of the model was that the occurrence of positive mortality is highly stochastic, and more likely to be driven by climate, drought, and stand characteristics than competition and community assembly (Trugman *et al.* 2021; Venturas *et al.* 2021). Moreover, explaining the difference between no mortality and any mortality

756 was of less interest than investigating the wide range of observed mortality rates which were greater
 757 than zero.

758 We included three penalized beta-splines in both components of the model on each of year, latitude,
 759 and longitude. The spline on year was included to account for large-scale temporal trends and
 760 reduce temporal autocorrelation in the residuals. Likewise, the splines on latitude and longitude
 761 were designed to capture unmeasured geospatial variation across the FIA dataset, and to account for
 762 spatial autocorrelation. We allowed 3 degrees of freedom for the temporal spline, and 18 degrees of
 763 freedom for each of the spatial splines. These values were chosen to allow sufficient flexibility in
 764 capturing the underlying relationships without overfitting to small-scale trends. The model was fit
 765 using the generalized additive models for location, scale, and shape (GAMLSS) framework, which
 766 allows for substantial flexibility in modeling parametric distributions using additive smoothers. The
 767 model was fit using the 'gamlss' package (version 5.4-22) in R (Stasinopoulos & Rigby 2007), and
 768 all predictors except year, latitude and longitude were normalized to standard units to aid model
 769 fitting and facilitate the comparison of effect sizes.

770 To estimate a combined effect of each covariate on mortality for both inference and visualization,
 771 we calculated the expected annualized mortality rate as $(1 - v_i)\mu_i$. The delta method was then used
 772 to calculate approximate standard errors and confidence intervals for the combined metric (Oehlert
 773 1992).

774 **6 Modeling growth response to drought**

Table S2: Growth Model Specification

Linear vs. Smooth	Variable
Linear	Tradeoff Strength
	Tradeoff Adherence
	CWM Drought Tol.
	CWM Resource Acq.
	Range Drought Tol.
	Range Resource Acq.
	Drought Strength
	Drought Burden
	Elevation
	MAP
	MAT
	Stand Age
	Basal Area
	Drought Strength x Basal Area

Continued on next page

Continued from previous page

Linear vs. Smooth	Variable
Smooth	Tradeoff Strength x Basal Area
	Tradeoff Adherence x Basal Area
	Latitude
	Longitude
	Year

775 To model growth response to drought, we fit a Gaussian generalized additive model for the relationship
 776 between annualized basal area growth rate and the same list of predictors used in the beta component of the mortality model. We again included three splines on year, latitude and longitude.
 777 Here we used penalized regression splines as implemented in the 'mgcv' package in R, allowing up
 778 to 10 knots for year, and 20 knots for both latitude and longitude. Covariates were again normalized
 779 to standard units before model fitting.

7 Sensitivity Analyses

781 One of our primary findings is that communities that more closely adhere to tradeoffs between drought tolerance and resource acquisitiveness experience lower mortality and faster basal area growth during drought. However, interpretation of this result could be complicated by collinearity between tradeoff adherence and the range of drought tolerance and resource acquisitiveness within communities. Some degree of correlation is expected, as tradeoff adherence reflects the dispersion of traits around the tradeoff, and communities spanning a wider range of trait values may exhibit greater spread. The correlation between tradeoff adherence and the range in drought tolerance was modest ($r = 0.12$), whereas the correlation with the range in resource acquisitiveness was stronger ($r = 0.38$). To assess the robustness of our results to this collinearity, we refit the mortality and growth models under two alternative specifications: (i) excluding both trait range variables while retaining tradeoff adherence, and (ii) excluding tradeoff adherence while retaining both trait range variables.

782 Excluding the range variables did not qualitatively alter results for either mortality or growth (Tables S8, S10). In the mortality model, the estimated effect of tradeoff adherence was nearly unchanged (0.023 [0.01, 0.037] versus 0.024 [0.012, 0.036]). In the growth model, removing the range variables strengthened the estimated effect of tradeoff adherence (-0.047 [-0.057, -0.036] versus -0.025 [-0.04, -0.01]), suggesting that tradeoff adherence absorbed part of the negative effect previously attributed to the range in resource acquisitiveness (Table S7). This result supports inclusion of both tradeoff adherence and trait range metrics in the full model, as omission of either may inflate the estimated effect of the other.

783 Similarly, excluding tradeoff adherence had little effect on the estimated impacts of trait ranges. In mortality models, estimated effects of the range in drought tolerance (-0.005 [-0.02, 0.01] versus -0.002 [-0.017, 0.012]) and the range in resource acquisitiveness (0.005 [-0.011, 0.02] versus 0.008

804 [-0.005, 0.022]) were largely unchanged (Table S9). The same pattern held for growth models, with
 805 minimal differences in estimated effects of drought tolerance range (-0.002 [-0.01, 0.01] versus
 806 -0.006 [-0.018, 0.006]) and resource acquisitiveness range (-0.05 [-0.06, -0.04] versus -0.049 [-0.061,
 807 -0.037]) when tradeoff adherence was excluded (Table S11). Together, these results indicate that
 808 collinearity between trait ranges and tradeoff adherence does not explain, nor substantially influence,
 809 the observed relationships between tradeoff adherence and forest mortality or growth during drought.

810 **8 Supplementary Tables**

Table S3: Tradeoff Strength by Ecoregion

Ecoregion	n	Mean	95% CI (lower)	95% CI (upper)
Central USA Plains	306	-2.17	-2.85	-1.31
Great Plains	1007	-1.14	-1.28	-0.79
Marine West Coast Forest	131	-1.51	-1.87	-0.78
Mediterranean California	61	-0.02	-0.20	0.51
Mississippi Alluvial And Southeast USA	493	-0.55	-1.06	-0.004
Coastal Plains				
Mixed Wood Plains	710	0.58	-2.29	0.69
North American Deserts	431	-1.83	-1.83	-1.83
Northern Forests	690	-2.50	-2.88	-1.87
Northwestern Forested Mountains	1234	-1.77	-1.82	-1.61
Ozark/Ouachita-Appalachian Forests	851	-1.99	-2.25	-1.71
Southeastern USA Plains	1607	-1.34	-1.45	-1.16
Temperate Sierras	144	-1.81	-1.82	-0.63

Table S4: Biophysical Drivers of Tradeoff Strength

Coefficient	Estimate	95% CI (lower)	95% CI (upper)
(Intercept)	-1.27	-1.64	-0.58
MAP	0.18	0.04	0.53
MAT	0.06	-0.17	0.16
Stand Age	-0.01	-0.17	0.02

Table S5: Biophysical Drivers of Tradeoff Adherence

Coefficient	Estimate	95% CI (lower)	95% CI (upper)
Continued on next page			

Continued from previous page

Coefficient	Estimate	95% CI (lower)	95% CI (upper)
(Intercept)	-1.48	-1.60	-1.40
map _{scaled}	0.31	0.19	0.41
mat _{scaled}	-0.29	-0.38	-0.19
stand _{agescaled}	-0.14	-0.29	0.05

Table S6: Full Mortality Model Results

Coefficient	Estimate	Std. Error	95% CI (lower)	95% CI (upper)
<u>μ component</u>				
(Intercept)	-4.771	0.153	-5.072	-4.470
BA	-0.095	0.007	-0.108	-0.081
Drought Strength	-0.039	0.006	-0.050	-0.028
Drought Burden	0.046	0.007	0.032	0.059
Tradeoff Strength	0.006	0.007	-0.007	0.019
Tradeoff Adherence	0.023	0.007	0.010	0.037
MAP	0.119	0.007	0.106	0.132
MAT	0.022	0.027	-0.032	0.077
CWM Drought Tol.	-0.025	0.008	-0.042	-0.009
CWM Resource Acq.	0.019	0.008	0.004	0.034
Range Drought Tol.	-0.005	0.008	-0.020	0.010
Range Resource Acq.	0.005	0.008	-0.011	0.020
Elevation	0.028	0.014	0.000	0.056
Stand Age	0.022	0.007	0.009	0.035
BA x Drought Strength	-0.008	0.006	-0.021	0.004
BA x Tradeoff Strength	-0.003	0.006	-0.014	0.009
BA x Tradeoff Adherence	0.002	0.006	-0.010	0.014
<u>ν component</u>				
(Intercept)	-6.255	0.323	-6.892	-5.618
BA	-0.260	0.013	-0.287	-0.234
Drought Strength	0.074	0.013	0.048	0.100
Drought Burden	0.020	0.014	-0.008	0.049
MAP	-0.010	0.015	-0.039	0.019
MAT	0.658	0.060	0.540	0.776
Elevation	-0.174	0.030	-0.234	-0.114
Stand Age	-0.075	0.015	-0.104	-0.046
BA x Drought Strength	0.031	0.014	0.004	0.058

Table S7: Full Growth Model Results

Coefficient	Estimate	Std. Error	95% CI (lower)	95% CI (upper)
(Intercept)	-0.173	0.022	-0.22	-0.13
BA	-0.260	0.006	-0.27	-0.25
Drought Strength	0.035	0.006	0.02	0.05
Drought Burden	0.014	0.007	0.00	0.03
Tradeoff Strength	-0.018	0.006	-0.03	-0.01
Tradeoff Adherence	-0.025	0.006	-0.04	-0.01
MAP	0.119	0.008	0.10	0.14
MAT	-0.027	0.031	-0.09	0.03
CWM Drought Tol.	-0.007	0.007	-0.02	0.01
CWM Resource Acq.	-0.026	0.008	-0.04	-0.01
Range Drought Tol.	-0.002	0.006	-0.01	0.01
Range Resource Acq.	-0.050	0.007	-0.06	-0.04
Elevation	-0.038	0.021	-0.08	0.00
Stand Age	-0.197	0.006	-0.21	-0.19
BA x Drought Strength	0.077	0.005	0.07	0.09
BA x Tradeoff Strength	-0.001	0.005	-0.01	0.01
BA x Tradeoff Adherence	-0.023	0.005	-0.03	-0.01

Table S8: Mortality Model (without trait range variables)

Coefficient	Estimate	Std. Error	95% CI (lower)	95% CI (upper)
μ component				
(Intercept)	-4.762	0.150	-5.059	-4.466
PB(year)	0.006	0.001	0.004	0.008
PB(lon)	0.005	0.001	0.003	0.006
PB(lat)	0.014	0.005	0.005	0.023
BA	-0.095	0.007	-0.108	-0.081
Drought Strength	-0.039	0.006	-0.050	-0.028
Drought Burden	0.046	0.007	0.032	0.059
Tradeoff Strength	0.004	0.006	-0.008	0.015
Tradeoff Adherence	0.024	0.006	0.012	0.036
MAP	0.119	0.007	0.106	0.133
MAT	0.022	0.027	-0.032	0.075
CWM Drought Tol.	-0.027	0.007	-0.041	-0.013
CWM Resource Acq.	0.019	0.008	0.004	0.034
Elevation	0.029	0.014	0.001	0.057
Stand Age	0.022	0.007	0.009	0.035

Continued on next page

Continued from previous page

Coefficient	Estimate	Std. Error	95% CI (lower)	95% CI (upper)
BA x Drought Strength	-0.008	0.006	-0.021	0.004
BA x Tradeoff Strength	-0.003	0.006	-0.014	0.008
BA x Tradeoff Adherence	0.002	0.006	-0.009	0.014
<u>v component</u>				
(Intercept)	-6.261	0.323	-6.898	-5.625
PB(year)	-0.030	0.002	-0.035	-0.026
PB(lon)	-0.035	0.001	-0.038	-0.032
PB(lat)	0.056	0.010	0.036	0.076
BA	-0.260	0.013	-0.286	-0.233
Drought Strength	0.075	0.013	0.049	0.101
Drought Burden	0.021	0.014	-0.007	0.049
MAP	-0.010	0.015	-0.039	0.019
MAT	0.660	0.060	0.541	0.778
Elevation	-0.172	0.030	-0.232	-0.112
Stand Age	-0.075	0.015	-0.104	-0.046
BA x Drought Strength	0.031	0.014	0.005	0.058

Table S9: Mortality Model (no tradeoff variables)

Coefficient	Estimate	Std. Error	95% CI (lower)	95% CI (upper)
<u>μ component</u>				
(Intercept)	-4.704	0.152	-5.003	-4.404
BA	-0.096	0.007	-0.109	-0.083
Drought Strength	-0.039	0.006	-0.050	-0.028
Drought Burden	0.046	0.007	0.033	0.060
MAP	0.117	0.007	0.104	0.130
MAT	0.021	0.027	-0.033	0.075
CWM Drought Tol.	-0.029	0.008	-0.045	-0.013
CWM Resource Acq.	0.018	0.008	0.003	0.033
Range Drought Tol.	-0.002	0.007	-0.017	0.012
Range Resource Acq.	0.008	0.007	-0.005	0.022
Elevation	0.029	0.014	0.002	0.057
Stand Age	0.022	0.007	0.009	0.036
BA x Drought Strength	-0.009	0.006	-0.021	0.003
<u>v component</u>				
(Intercept)	-6.261	0.323	-6.898	-5.625
BA	-0.260	0.013	-0.286	-0.233
Drought Strength	0.075	0.013	0.049	0.101

Continued on next page

Continued from previous page

Coefficient	Estimate	Std. Error	95% CI (lower)	95% CI (upper)
Drought Burden	0.021	0.014	-0.007	0.049
MAP	-0.010	0.015	-0.039	0.019
MAT	0.660	0.060	0.541	0.778
Elevation	-0.172	0.030	-0.232	-0.112
Stand Age	-0.075	0.015	-0.104	-0.046
BA x Drought Strength	0.031	0.014	0.005	0.058

Table S10: Growth model (without trait range variables)

Coefficient	Estimate	Std. Error	95% CI (lower)	95% CI (upper)
(Intercept)	-0.173	0.023	-0.218	-0.128
BA	-0.261	0.006	-0.272	-0.250
Drought Strength	0.035	0.006	0.024	0.046
Drought Burden	0.014	0.007	0.000	0.027
Tradeoff Strength	0.003	0.005	-0.007	0.014
Tradeoff Adherence	-0.047	0.005	-0.057	-0.036
MAP	0.121	0.008	0.104	0.138
MAT	-0.019	0.031	-0.079	0.042
CWM Drought Tol.	-0.013	0.006	-0.026	-0.001
CWM Resource Acq.	-0.026	0.008	-0.042	-0.010
Elevation	-0.038	0.021	-0.079	0.003
Stand Age	-0.197	0.006	-0.209	-0.186
BA x Drought Strength	0.077	0.005	0.067	0.087
BA x Tradeoff Strength	0.000	0.005	-0.009	0.009
BA x Tradeoff Adherence	-0.023	0.005	-0.033	-0.014

Table S11: Growth Model (without tradeoff variables)

Coefficient	Estimate	Std. Error	95% CI (lower)	95% CI (upper)
(Intercept)	-0.158	0.021	-0.199	-0.116
BA	-0.252	0.005	-0.263	-0.242
Drought Strength	0.034	0.006	0.023	0.045
Drought Burden	0.013	0.007	0.000	0.027
MAP	0.127	0.008	0.110	0.143
MAT	-0.028	0.031	-0.089	0.032
CWM Drought Tol.	-0.002	0.007	-0.015	0.011
CWM Resource Acq.	-0.024	0.008	-0.040	-0.008

Continued on next page

Continued from previous page

Coefficient	Estimate	Std. Error	95% CI (lower)	95% CI (upper)
Range Drought Tol.	-0.006	0.006	-0.018	0.006
Range Resource Acq.	-0.049	0.006	-0.061	-0.037
Elevation	-0.042	0.021	-0.083	-0.001
Stand Age	-0.197	0.006	-0.208	-0.186
BA x Drought Strength	0.081	0.005	0.070	0.091